



**Sérgio Manuel
Rodrigues dos Santos**

**Caracterização do processo de recuperação de
metanol na Prio Biocombustíveis S.A.**

**Characterization of the methanol recovery process
at Prio Biocombustíveis S.A.**



**Sérgio Manuel
Rodrigues dos Santos**

**Caracterização do processo de recuperação de
metanol na Prio Biocombustíveis S.A.**

**Characterization of the methanol recovery process
at Prio Biocombustíveis S.A.**

Dissertação apresentada à Universidade de Aveiro para cumprimento dos requisitos necessários à obtenção do grau de Mestre em Engenharia Química, realizada sob a orientação científica do Doutor Francisco Avelino da Silva Freitas, Professor do Departamento de Química da Universidade de Aveiro, e Engenheira Anabela Ferreira Antunes, Diretora de Produção - Direção de Gestão de Projetos e Sustentabilidade - Prio Biocombustíveis S.A.

Júri / Jury

Presidente / President

Maria Inês Purcell de Portugal Branco

Professora Auxiliar do Departamento de Química da Universidade de Aveiro

Vogais / Examiners committee

Marco Paulo Seabra dos Reis

Professor Auxiliar do Departamento de Engenharia Química da Faculdade de Ciências e Tecnologia da Universidade de Coimbra

Anabela Ferreira Antunes

Diretora de Produção - Direção de Gestão de Projetos e Sustentabilidade - Prio Biocombustíveis S.A.

Agradecimentos / Acknowledgements

Quero agradecer aos meus pais pela oportunidade de ter acesso a uma educação superior e às minhas irmãs pelo constante incentivo dado ao longo da minha jornada educacional. Agradeço também à minha namorada Rita pelo apoio incondicional dado durante todo o meu percurso universitário e por ter tornado esta jornada mais fácil e agradável.

Ao Prof. Doutor Francisco Avelino e Eng^a Anabela Antunes pela orientação e conhecimentos transmitidos.

À Prio Biocombustíveis pela oportunidade dada para a realização deste trabalho e a todos seus colaboradores pelo suporte e simpatia e em particular à Eng^a Lídia Pascoal que me guiou durante a fase experimental deste trabalho.

Não poderia deixar de agradecer a todos os meus amigos, em particular ao Ivo, pela ajuda e companheirismo, e ao Cristofe, Joana, Marta, Ana Arede, Ana Patrícia, Tânia, Ana Filipa, Micaela, Sofia e muitos outros, por terem marcado a minha jornada com momentos memoráveis e de camaradagem incondicional.

Palavras-chave

Metanol, Simulação de Processo, Análise aos Componentes Principais, Desenho de Experiências, Regressão linear Múltipla, Fouling.

Resumo

Em ambiente industrial, conhecer o processo em que se está a trabalhar é crucial para assegurar o seu bom funcionamento. No presente trabalho, desenvolvido nas instalações da Prio Biocombustíveis, utilizando dados do processo, recolhidos no decorrer do trabalho, e dados do histórico de produção caracterizou-se o processo de recuperação de metanol, tendo-se começando pela caracterização das correntes chave do mesmo. Com base na informação obtida na caracterização de correntes, o software de simulação de processos químicos Aspen Plus® foi utilizado para replicar o processo e realizar uma análise de sensibilidade com o fim de discernir a importância relativa de variáveis chave do processo (rácio refluxo/alimentação, temperatura de refluxo, temperatura à saída do reboiler, composições na alimentação de metanol, glicerol e água). O trabalho continuou com a aplicação de um conjunto de ferramentas estatísticas, começando pela Análise aos Componentes Principais onde se estudaram as interações entre variáveis e a sua contribuição para a variabilidade do processo. De seguida, o método de Desenho de Experiências foi utilizado para obter dados experimentais para com eles criar um modelo capaz de simular a quantidade de água no destilado. No entanto, para este método, as condições necessárias à sua realização não se verificaram, levando ao seu abandono. Passou-se então para o método de Regressão Linear Múltipla, utilizando dados observacionais, do qual surgiram vários modelos empíricos, o melhor apresentando um R^2 igual a 92.93% a AARD igual a 19.44%. Apesar de o AARD ainda ser relativamente alto, considera-se que o modelo é adequado para realizar estimativas rápidas da condição do destilado na coluna. A influência do fouling no processo foi também muitas vezes notada ao longo deste trabalho. Não sendo possível a medição direta do fouling no processo, a pressão do vapor à entrada do reboiler foi usada como indicador do estado do fouling, tendo sido utilizada para estudar o desenvolvimento do fouling e a influência da quantidade de UCO, incorporado no processo, na sua formação. Quando se compara o custo do vapor associado à operação do reboiler, quando a coluna opera com fouling (3 bar de pressão de vapor), ou sem fouling (1.5 bar de pressão de vapor), verifica-se um aumento de cerca de 58% nos custos para o caso em que o fouling é maior.

keywords

Methanol, Process simulation, Principal Components Analysis, Design of experiments, Multiple linear Regression, Fouling.

Abstract

In a industrial environment, to know the process one is working with is crucial to ensure its good functioning. In the present work, developed at Prio Biocombustíveis S.A. facilities, using process data, collected during the present work, and historical process data, the methanol recovery process was characterized, having started with the characterization of key process streams. Based on the information retrieved from the stream characterization, Aspen Plus® process simulation software was used to replicate the process and perform a sensitivity analysis with the objective of accessing the relative importance of certain key process variables (reflux/feed ratio, reflux temperature, reboiler outlet temperature, methanol, glycerol and water feed compositions). The work proceeded with the application of a set of statistical tools, starting with the Principal Components Analysis (PCA) from which the interactions between process variables and their contribution to the process variability was studied. Next, the Design of Experiments (DoE) was used to acquire experimental data and, with it, create a model for the water amount in the distillate. However, the necessary conditions to perform this method were not met and so it was abandoned. The Multiple Linear Regression method (MLR) was then used with the available data, creating several empiric models for the water at distillate, the one with the highest fit having a R^2 equal to 92.93% and AARD equal to 19.44%. Despite the AARD still being relatively high, the model is still adequate to make fast estimates of the distillate's quality. As for fouling, its presence has been noticed many times during this work. Not being possible to directly measure the fouling, the reboiler inlet steam pressure was used as an indicator of the fouling growth and its growth variation with the amount of Used Cooking Oil incorporated in the whole process. Comparing the steam cost associated to the reboiler's operation when fouling is low (1.5 bar of steam pressure) and when fouling is high (reboiler's steam pressure of 3 bar), an increase of about 58% occurs when the fouling increases.

Contents

Contents	i
Nomenclature	iii
List of Figures	v
List of Tables	vii
1 Introduction	1
2 Biorefineries: a sustainable industry	3
2.1 The concept of Biorefinery	3
2.2 Biodiesel - example of a reliable biorrefinery	5
2.2.1 Biodiesel production methods	6
2.2.2 Raw materials	7
3 Prio Biocombustíveis S.A.	9
3.1 Biodiesel production process	9
3.1.1 Oil neutralization/degguming	10
3.1.2 Oil Transesterification	11
3.1.3 Methyl Esters washing	11
3.1.4 Methanol Recovery	12
3.1.5 Glycerol purification	15
3.2 An improvement driven industry	15
4 Process data: stream analysis and characterization	17
4.1 Stream composition	18
5 Modelling of the methanol recovery column with Aspen Plus®	21
5.1 Thermodynamic model parameters	22
5.2 Simulation results	24
5.3 Sensitivity analysis	26

6	Methanol recovery process models	35
6.1	PCA	35
6.2	Distillate purity	39
6.2.1	Design of Experiments	40
6.2.2	Multiple Linear Regression	41
6.3	Fouling and steam consumption	45
6.3.1	Operating costs associated with fouling	47
7	Conclusions and future work	49
	Bibliography	51
A	Glycerol and FAME vapour pressure	A1
B	Stream compositions and column's operating data	A3

Nomenclature

Acronyms

AARD Absolute average relative deviations

CIP Clean-in-place

DoE Design of Experiments

FAME Fatty acid methyl ester

MLR Multiple Linear Regression

MPC Model Predictive Control

PC Principal Components

PCA Principal Components Analysis

UCO Used Cooking Oil

UNIFAC UNiversal QUAsiChemical Functional-group Activity Coefficients model

UNIQUAC UNiversal QUAsiChemical model

Greek Symbols

β Regression coefficient

ε Random error component

Ξ_i Variable i w

Re Heat transfer resistance k/W

Subscripts

A stream A

B stream B

C	stream C
D	stream D
gly	glycerol
met	methanol
oth	“others”
steam	Process steam
tot	total
wtr	water

Symbols

v_k	Regressing variable	
ΔL	Material’s thickness	m
ΔT	Temperature difference between cold and hot side	K
Q	Mass flow	kg · h ⁻¹
R^2	Coefficient of determination	
x	Mass fraction	%
A	Heat transfer area	m ²
k	Material’s thermal conductivity	W/m ² · K
q	Heat flux	W

List of Figures

2.1	Petro and Bio-refinery comparison.	4
2.2	General process diagram for a biodiesel production plant.	6
3.1	Schematic representation of the neutralisation/deguming process at Prio Biocombustíveis S.A.	10
3.2	Schematic representation of the oil transesterification process at Prio Biocombustíveis S.A.	11
3.3	Schematic representation of the methyl esters washing process at Prio Biocombustíveis S.A.	12
3.4	Schematic representation of the methanol recovery process at Prio Biocombustíveis S.A.	13
3.5	a) Distillation column's reboiler head; b)Reboiler's pipes closeup.	14
3.6	Schematic representation of the glycerol purification process at Prio Biocombustíveis S.A.	15
4.1	Composition of stream A in % (wt)	19
4.2	Composition of stream D in % (wt)	19
4.3	Composition of stream C in % (wt)	20
4.4	Reboiler's steam pressure variation with time.	20
5.1	Aspen Plus [®] Flowsheet diagram used to simulate the distillation column with the RadFrac model.	22
5.2	Second liquid phase composition along the column, computed with Aspen Plus [®] , using the software's estimated UNIQUAC binary interaction parameters.	23
5.3	First liquid phase composition along the column, computed with Aspen Plus [®] , using the software's UNIQUAC binary interaction parameters.	24
5.4	Second liquid phase composition along the column, computed with Aspen Plus [®] using the user estimated UUNIQUAC binary interaction parameters.	24

5.5	Vapour phase composition along the column, computed with Aspen Plus® using UNIQUAC parameters estimated by the user.	25
5.6	Distillation column's temperature profiles.	28
5.7	Variation of the methanol mass fraction at the distillate with the variation of the reflux/feed ration.	28
5.8	Variation of the methanol mass fraction at the distillate with the variation of the reboiler outlet temperature.	30
5.9	Variation of the methanol mass fraction at the distillate with the variation of the reflux temperature.	31
5.10	Variation of the methanol mass fraction at the distillate with the variation of water amount in the feed stream.	31
5.11	Variation of the methanol mass fraction at the distillate with the variation of the methanol amount in the feed stream.	32
5.12	Variation of the methanol mass fraction at the distillate with the variation of the glycerol amount in the feed stream.	32
6.1	Loadings plot of the variables in the methanol distillation process PCA for the first three PCs.	38
6.2	PV/FF variation with the reboiler operating time.	46
6.3	Maximum reboiler operating time variation with the UCO percentage used in the production process.	47
B.1	Distillation column with the different temperature and pressure indicators relative location along the column.	A3

List of Tables

2.1	Targets for percentage biodiesel incorporation in transportation fuels in the EU and USA [10, 7]	5
2.2	Comparative table between the different transesterification methods [19, 20] .	7
2.3	Fatty acids composition of several vegetable and animals oils and used cooking oil.	8
4.1	Analytical methods used.	18
5.1	UNIQUAC binary interaction parameters used in the simulation.	26
5.2	Aspen Plus [®] simulation results corresponding to the 8th of April.	27
5.3	Comparison between the Aspen Plus [®] given compositions and the compositions observed in the field (% wt/wt) for streams C and D.	29
5.4	Equations, and respective derivatives, from the fitted data for each variable in study.	33
6.1	Eigenvalue and commutative variability for the methanol distillation process PCA.	36
6.2	Principal Components coefficients for the variables of the methanol recovery process.	37
6.3	Water on distillate results for the 2^2 factorial design of experiment for T102407 temperatures of 79°C and 82°C and for reflux/feed ratios of 33 and 37. $T_{7,obs}$ and R/FF_{obs} represent the true values of T102407 and reflux/feed registered during the experiment.	40
6.4	Water on distillate results for the 3^2 factorial design of experiment for T102407 temperatures of 78°C, 80°C and 82°C and for reflux/feed ratios of 0.32, 0.34 and 0.36. $T_{7,obs}$ and R/FF_{obs} represent the true values of T102407 and reflux/feed registered during the experiment.	41
6.5	MLR results for the water on distillate model, using reflux/feed ratio and thermocouple's temperature T102407.	43

6.6	MLR results for the water on distillate model, using reflux/feed ratio and thermocouple's temperature T102405.	44
6.7	Steam flow and pressure values used to regress equation 6.7.	47
A.1	Antoine equation parameters	A2
B.1	Mass fraction composition (%) of glycerol, water, methanol and "others" in Stream A (from tank 10F08)	A4
B.2	Mass fraction composition (%) of glycerol, water, methanol and "others" in Stream D (from the bottom of the distillation column)	A5
B.3	Mass fraction composition (%) of water and methanol in Stream C (from tank 10F06)	A7
B.4	Methanol distillation column's operating data.	A8
B.5	Column's thermocouples T102404, T102405, T102406, T102407, T102408 and T102509 temperatures.	A10
B.6	Column's thermocouple T102403, feed and reflux temperatures and reboiler's steam (P102405) and internal pressures (P102401).	A11
B.7	Boiler steam production and respective daily energy consumption.	A13

Chapter 1

Introduction

Biodiesel is currently in increasing demand worldwide as a result of the growing commitment to find alternative green fuels. Transesterification production processes, as one of the methods to produce methyl esters, have also been the subject of continuous studies and improvements, with industrial plants striving more and more to achieve higher process efficiencies.

The present document is a Master's thesis, carried out in the scope of the Integrated Master's Degree in Chemical Engineering from University of Aveiro, and its objectives were the study of the methanol recovery process from Prio Biocombustíveis S.A. methyl ester transesterification plant, located in Terminal de Granéis Líquidos at Porto de Aveiro.

The main objectives for this work can be summarized as follows:

- Characterization of the methanol recovery process currents and development of a computerized model to simulate it;
- Sensitivity analysis of key variables in the methanol recovery process and the study of the process variables importance and relations;
- Development of an empiric model to predict the water content in the methanol distillate;
- Study the effect of fouling in the reboiler and create a model to predict the fouling evolution during production.

With the present work, new information regarding the methanol distillation process as well as a new set of tools were developed for Prio Biocombustíveis, allowing the company's workers to better understand and control the production process.

This work is divided in seven chapters:

- Chapter 2 briefly discusses the Biorefineries concept and the biodiesel production industry, presenting the different production methods and its raw materials;

-
- Chapter 3 contains a more detailed description of the several production stages of Prio Biocombustíveis S.A. production process;
 - Chapter 4 presents the analytical methods used to characterize the process currents and respective results;
 - Chapter 5 deals with the computerized model to simulate the methanol distillation process, paying special attention to the importance of thermodynamic models in the simulation. It also contains a sensitivity analysis made to key process variables;
 - Chapter 6 holds the PCA analysis made to study the importance and relations of the process variables as well as the models created for the water content in distillate and reboiler's fouling;
 - Chapter 7 summarizes the present work's conclusions and indications regarding future works.

Chapter 2

Biorefineries: a sustainable industry

The perception that the planet's resources are limited and can be depleted, if explored at a higher rhythm than they regenerate, is already widespread through the industrialized world. This lead to the search for solutions, from which the following two stand [1]:

- Dematerialisation (use less resources, create less waste)
- Transmaterialisation (replace the current raw materials for others more sustainable)

Although dematerialisation is easier to implement by both industry and consumers, it's results aren't always the expected since it requires constant improvement of the production processes, that developing countries don't make the same mistakes developed countries did and also because this idea focus on reducing the consumption and doesn't take into account the waste that is still created and many times disposed of and not yet recycled [1]. As for transmaterialisation, it poses a more sustainable approach as it focus not in reducing the consumption but in an adaptation of its limits to the limits at which the resources can regenerate and in reusing and recycling the materials as much as possible to create a circular economy [2].

The energy industry, in which the fuel industry is inserted, is no exception to what was said before, especially because of it's dependency towards fossil fuels (oil in particular) which are becoming more scarce and will eventually be unable to provide the for the growing demand of liquid fuels [3]. This creates the perfect environment for the development and growth of alternative fuels, in particular those derived from biomass, a renewable (not unlimited) source that can be obtained from various sources such as agriculture (crops and residues), forestry, industry and households (waste and leftovers) and aquaculture (algae and seaweeds) [4].

2.1 The concept of Biorefinery

A biorefinery can be seen as a sustainable relative of an oil refinery, as showed in figure 2.1, the main difference between the two being the raw material it used: biomass - one of the

2.1. THE CONCEPT OF BIOREFINERY

most precious and versatile resources on Earth [5]. A biorefinery is defined as an industrial plant in which biomass is converted into a large variety of chemicals, biomaterials and energy, maximizing biomass's value while creating the minimal amount of waste [1].

Even though nowadays biorefineries's main focus is energy, it is expectable that in the future, due to developments in the area, they will increasingly produce a wider range of products, such as chemicals (ex: furfural, fatty and acetic acids, etc) and materials (ex: paints, dyes, biopolymers, etc), in considerable amounts [6].

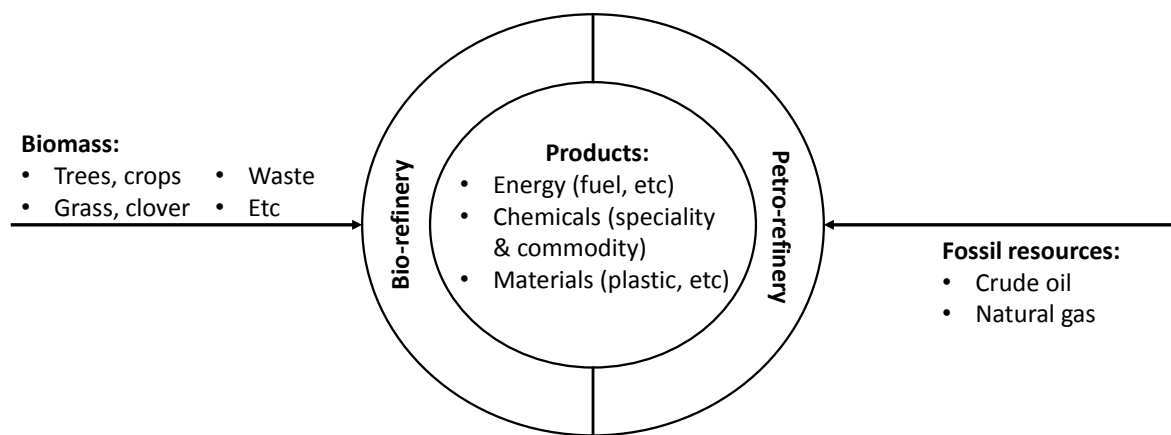


Figure 2.1: Petro and Bio-refinery comparison.

As is described in the literature [7], three different types of biorrefineries can be identified, based on its inputs and outputs:

- Type I - uses only one type of feedstock to yield a major product. It's the least flexible of the three.
- Type II - uses only one type of feedstock to yield several products.
- Type III - can use various types of feedstock to yield several products. It's the most flexible of the three.

Due to type III high flexibility and adaptability to use different raw materials and produce different products, in accordance with current market demands, this type of biorrefinery is in clear advantage regarding the other two. It is also of note that a biorrefinery can be classified according to the origin of the raw materials and processing technology it uses: the whole-crop biorrefinery (uses cereals or maize), the green biorrefinery (uses wet biomass) and the lignocellulose feedstock (LCF) biorrefinery (uses naturally dry cellulose-containing biomass and wastes) being the most researched and developed [7].

2.2 Biodiesel - example of a reliable biorrefinery

Biodiesel is a complex mixture of mono-alkyl esters obtained by transesterification of fatty acids from triglycerides with a short chain alcohol such as methanol or ethanol or by esterification of fatty acids [8]. It is an alternative diesel fuel that has renewable biological resources, such as vegetable oils and animal fats, as its precursor, being an excellent replacement to conventional fuels for diesel engines [5].

This type of fuel has the advantage of being biodegradable and non-toxic, having lower emission profile than fossil fuels [5, 9] and of containing very small quantities of sulphur, polycyclic aromatic hydrocarbons, and metals [8]. Apart from the environmental advantages, others come from the use of biodiesel such as its use in regular diesel engines without requiring any major engine modification, it is safe for storage and transportation due to its low amount of polycyclic aromatic hydrocarbons, it contains oxygen which makes it a better lubricant than regular diesel fuels (increasing the life span of engines), it's combustion is more complete and has a higher flash point which makes it safer to handle [5, 8]. For these reasons, an increase in biodiesel incorporation in regular fuels has been registered both in Europe and United States of America, as can be seen in table 2.1. In Portugal, the current percentage of biodiesel incorporation in regular fuels reached, early in 2015, the 7% mark.

Table 2.1: Targets for percentage biodiesel incorporation in transportation fuels in the EU and USA [10, 7]

year	2001	2004	2005	2010	2015	2020	2030
USA	-	0.50%	-	4%	-	10%	20%
EU	1.40%	-	2.50%	5.75%	7%	10%	-

Despite all of its advantages and it's promise as a fossil fuel replacement, biodiesel is still far from being able to completely replace fossil fuels in a near future as there are several challenges that need to be overcome first. One is it's price, as biodiesel cost is higher than that of petroleum diesel due to its raw material's price [5]. Another problem that needs to be overcome is the crying fact that this industry's demand for raw materials, being vegetable oils such as palm, rapeseed, soy and corn oil, increases the pressure for its production which, in turn, leads to an increase in deforestation and serious food shortages [8, 11].

The use of other feedstocks, such as waste cooking oils, is already implemented [12, 13, 14]. Even though using this type of oil to produce biodiesel can, in part, help solving the problems of food shortage and deforestation, new production problems arise like the higher content of free fatty-acids and water that increase the soap production in the presence of an alkali-catalyst [8]. Algae is another promising source of biomass for biodiesel as they can grow practically anywhere where there is enough sunshine (salt water environments included). Algae have a short growing cycle of only a few days and yield an amount of oil that is several

times larger than that of the best performing crops [5, 8, 15], thus translating into a smaller impact on both environment and food markets.

According to the feedstock used in it's production, biodiesel can be classified as [16]:

- First generation biodiesel - biodiesel produced from edible oils (example: palm, soy and corn oil)
- Second generation biodiesel - biodiesel produced from non-edible oils (example: jatropha, mahua and jojoba oil)
- Third generation biodiesel - biodiesel produced from microalgae oils

2.2.1 Biodiesel production methods

The process of biodiesel production is not as new as one might think since s early as 1853 scientists E. Duffy and J. Patrick performed transesterification experiments and even before World War II transesterified vegetable oils were used to power heavy-duty vehicles in South Africa. [17]. However, it was only in the late 90s that production and commercialisation of biodiesel really took off [5]. The major stages in biodiesel production are crude oil degumming, refining and drying, followed by transesterification and alkyl esters (biodiesel) separation, alkyl esters washing and drying, alcohol recovery and glycerol purification [18]. In figure 2.2 a schematic of the major stages in a biodiesel production plant are shown.

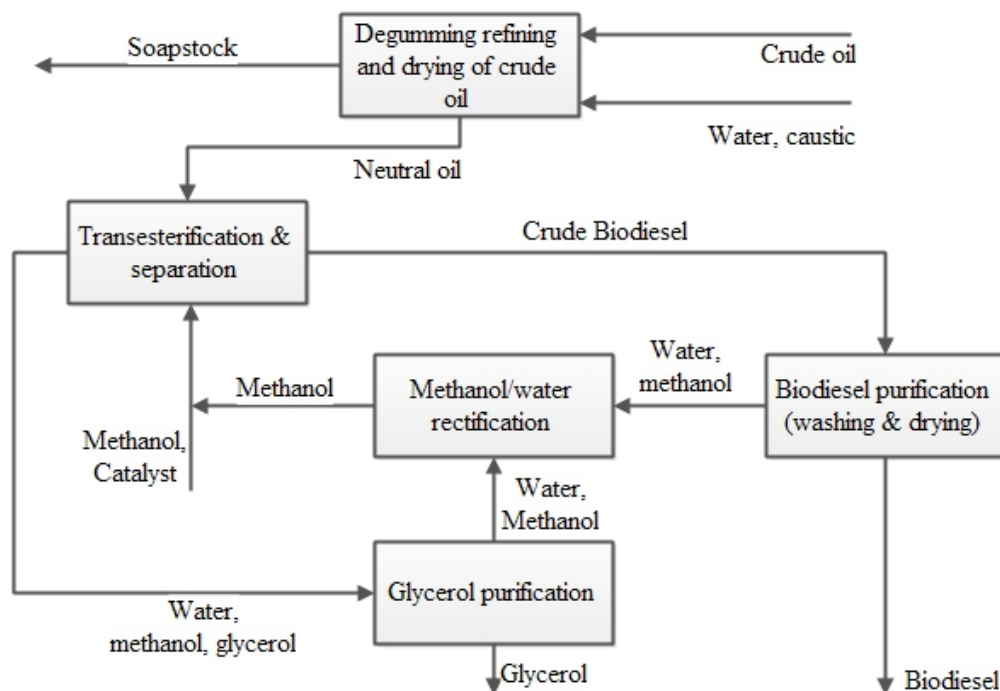
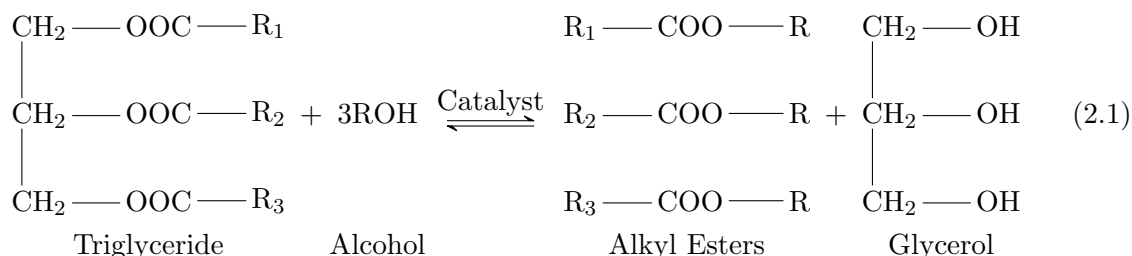


Figure 2.2: General process diagram for a biodiesel production plant.

A transesterification reaction consists in the reaction of a triglyceride molecule with a

primary or secondary short chain monohydric aliphatic alcohol (1-8 carbons), in the presence of a suitable catalyst, to yield 3 monoalkyl esters and glycerol (the main by-product) as is shown in equation 2.1.



Regarding the catalysts used in the process of transesterification, they can either be alkali (such as sodium or potassium hydroxide or sodium methoxide), acid (such as sulfuric, hydrochloric and sulfonic acids) or enzyme. Apart from the catalysed processes, another route for this reaction is the non-catalysed supercritical alcohol transesterification [5, 19]. A comparison between the different transesterification methods is presented in table 2.2.

Table 2.2: Comparative table between the different transesterification methods [19, 20]

	Alkali-catalyst	Acid-catalyst	Lipase-Catalyst	Supercritical alcohol
Reaction temperature (°C)	60-70	55-80	30-40	239-385
Reaction pressure (MPa)	0.1	0.1	0.1	10-25
Reaction time (min)	60-360	60-360	60-360	7-15
Free fatty acids in raw materials	Saponified products	Esters	Esters	Esters
Water in raw materials	Interference with reaction	Interference with reaction	No influence	-
Yield of methyl esters	Normal	Normal	Higher	Good
Recovery of glycerol	Difficult	Difficult	Easy	-
Purification of methyl esters	Repeated washing	Repeated washing	None	-
Production cost of catalyst	Cheap	Cheap	Relatively expensive	Medium

2.2.2 Raw materials

The raw material for the biodiesel industry are oils which, has seen before, can be of very different sources and regions of the globe, thus differing in their composition, as shown in

table 2.3. Regarding vegetable oils, they are extracted from seeds and are mainly comprised of glycerides (try, di and monoglycerides) and, in lesser quantities, by other compounds like tocopherols, sterols, sterol esters, phosphatides, free fatty acids, odours, colouring matter, waxes and metal compounds [5, 21]. Used cooking oil (UCO) is also used in the biodiesel industry as cheaper raw material. Triglycerides are the major constituents of vegetable oils [22] as well as the main precursor for mono-alkyl esters. They are esters of three fatty acids and one glycerol, having in its structure a substantial amount of oxygen and its fatty acids varying in their carbon chain length and number of double bonds.

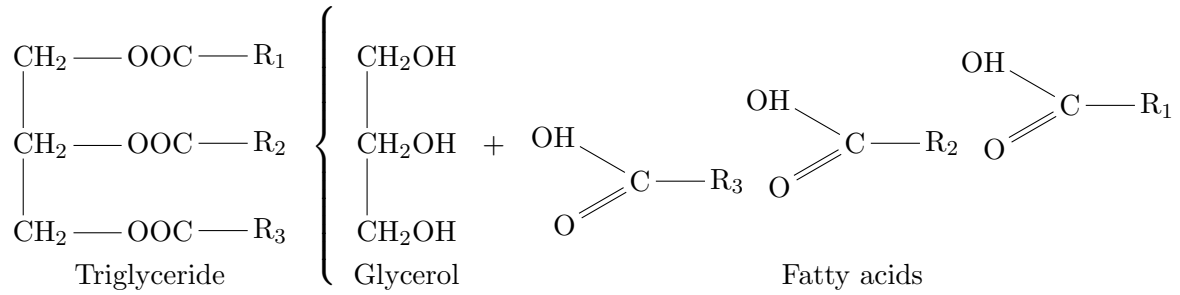


Table 2.3: Fatty acids composition of several vegetable and animals oils and used cooking oil.

Fatty acids	Fatty acids composition (wt%)							
	Oil							
	corn ^a	rapeseed ^a	soy ^a	palm ^b	peanut ^a	tallow ^b	lard ^b	UCO ^c
lauric (12:0 ^d)	0	0	0	0.1	0	0.1	0.1	-
myristic (14:0 ^d)	0	0	0	1	0	2.8	1.4	-
palmitic (16:0 ^d)	12	3	12	42.8	11	23.3	23.6	6.8
stearic (18:0 ^d)	2	1	3	4.5	2	19.4	14.2	3.7
arachidic (20:0 ^d)	Tr	0	0	-	1	-	-	-
behenic (22:0 ^d)	0	0	0	-	2	-	-	-
lignoceric (24:0 ^d)	0	0	0	-	1	-	-	-
palmitoleic (16:1 ^d)	-	-	-	-	-	-	-	0.4
oleic (18:1 ^d)	25	64	23	40.5	48	42.4	44.2	22.8
erucic (22:1 ^d)	0	0	0	-	0	-	-	-
linoleic (18:2 ^d)	6	22	55	10.1	32	2.9	10.7	65.2
linolenic (18:3 ^d)	Tr	8	6	0.2	1	0.9	0.4	0.1

Tr stands for traces.

^a data acquired from A. Srivastava *et al*, 2000[22]

^b data acquired from F. Ma *et al*, 1999[9].

^c data acquired from A. Demirbas, 2009[23].

^d common notation for fatty acids (carbon number:number of double links)

Chapter 3

Prio Biocombustíveis S.A.

Prio Biocombustíveis S.A. is a biodiesel production company created in 2006 and is sited in Terminal de Granéis Líquidos at Porto de Aveiro, having a production capacity of 113880 ton/year. Apart from biodiesel, glycerol, a secondary product of the Transesterification process, is also commercialised.

The biodiesel produced here is in conformity with the European Standards described in EN14214, the company being also certified in Quality (ISO 9001), Safety (OHSAS 18001) and Environment (ISO 14001).

3.1 Biodiesel production process

The production of biodiesel at Prio Biocombustíveis S.A, which will explain here, is the alkaline transesterification of vegetable and used cooking oils, according to the Lurgi process [24].

The crude oil quality (which can be soy, palm, rapeseed or used cooking oil) is one of the parameters that influence the most the production process, being required that the oils are tested, at arrival, for water and free fatty acids (FFA) content even before they start being processed to ensure that water and FFAs levels are within acceptable limits. This step is of the most importance to ensure that both yield and quality of the biodiesel produced are high, with special attention to UCO since it can have high levels of both water and FFAs [12, 25] and also to allow the determination of sodium hydroxide quantity to be added in the neutralization/deguming stage.

Apart from used cooking oil, which is used all year long, the vegetable oils used for the production of biodiesel vary from soy oil, rapeseed oil and palm oil. The choice of vegetable oil to be used, or mixtures of them, is largely defined by market prices, specific oil properties and by clients specification. While soy and rapeseed oils are used during the winter, palm oil, due to its higher viscosity and crystallization at low temperatures [26, 27], is only used during summer time.

3.1.1 Oil neutralization/degumming

Prior testing, the crude oil mixture is fed to the neutralization/degumming process where it's transformed into neutral oil, so called due its low FFAs and other impurities content. In this step, the crude oil is initially heated following the removal of metals and non-hydratable phosphatides (NHP), such as phosphatide acid, by adding phosphoric acid[21]. A sodium hydroxide solution is added next to react with the FFAs to form soaps (saponification) and other impurities that weren't removed with the addition of the phosphoric acid [18]. After both phosphoric acid and sodium hydroxide addition, the mixture is centrifuged to separate the soaps and small quantities of metals and other precipitates (soapstock). Finally, water is added to wash any remnants of soap and soluble impurities from the oil, being then removed in the second centrifuge. The resulting oil is dried and proceeds for the transesterification process as neutral oil. A schematic representation of the neutralisation/degumming process is given at figure 3.1.

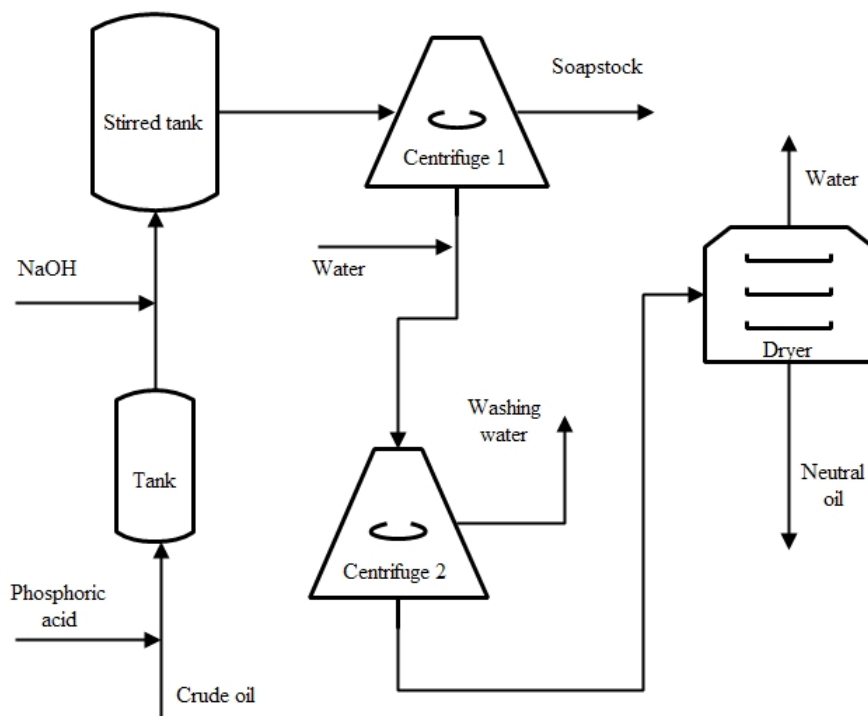


Figure 3.1: Schematic representation of the neutralisation/degumming process at Prio Biocombustíveis S.A.

The oil neutralization/degumming is crucial in the transesterification reaction since high levels of FFAs will result in catalyst destruction and soap formation, leading to lower alkyl esters yield, inhibiting the alkyl esters and glycerol separation and contributing to the formation of an emulsion during biodiesel washing [12]. The water used in the oil washing step is slightly acid to allow for a more complete removal of soaps [28].

3.1.2 Oil Transesterification

Oil transesterification to alkyl esters at Prio Biocombustíveis S.A. is made by alkaline catalysis using sodium methoxide as catalyst and methanol as the alcohol. The neutral oil is fed to the first reactor, along with the catalyst and methanol, yielding methyl esters of the corresponding fatty acids present in the oil's triglycerides. Methanol is used in a higher quantity than the stoichiometric quantity required for the complete reaction to force the equilibrium of equation 2.1 towards the products [9, 12, 18].

Even with the excess methanol, the reaction in the first reactor is not complete and a second reactor is used to carry the reaction even further, for a near complete oil conversion. The reaction mixture from the first reactor follows to a decanter where the glycerol phase is separated from the rest of the mixture, the later being fed to the second reactor. The products from the second reactor are also fed to a decanter where, like in the first, the glycerol phase formed is separated. Both reactors are separated in 3 internal individual stirred compartments for a more efficient stirring. The glycerol removed from the first decanter follows for further purification while the glycerol stream from the second decanter is recycled to the first reactor, following Lurgi's glycerol cross flow production method [24]. A Schematic representation of the oil transesterification process at Prio Biocombustíveis S.A. is presented in figure 3.2.

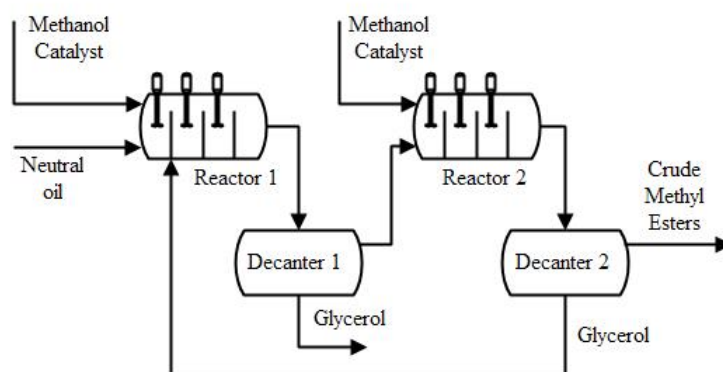


Figure 3.2: Schematic representation of the oil transesterification process at Prio Biocombustíveis S.A.

3.1.3 Methyl Esters washing

After the transesterification stage is complete, the crude methyl esters mixture (crude biodiesel) from the the second decanter still contains a small amount of impurities such as catalyst, soaps, glycerol and methanol, requiring further purification. Accordingly, the crude biodiesel goes through a liquid-liquid separation column where it is washed with slightly acid water, leading to methanol, glycerol, salts and soaps being transferred from the biodiesel to the aqueous phase [12, 18]. The water used contains hydrochloridric acid that reacts

with soaps, thus preventing the formation of foam. The washed biodiesel is then dried to remove residual water and methanol, after which it follows for additization. A schematic representation of the methyl esters washing process at Prio Biocombustíveis S.A. is shown in figure 3.3.

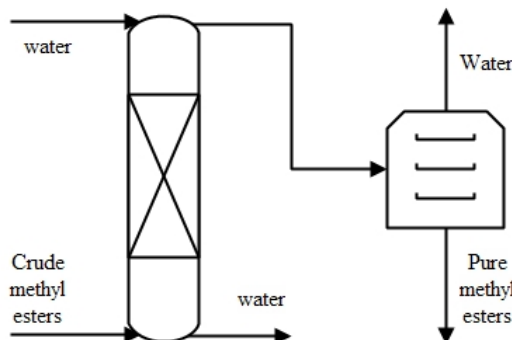


Figure 3.3: Schematic representation of the methyl esters washing process at Prio Biocombustíveis S.A.

3.1.4 Methanol Recovery

Methanol, as explained in 3.1.2, is used in excess during the transesterification process and needs to be recovered, hence the need of a methanol recovery process which is schematically represented in figure 3.4. This process is performed (at Prio Biocombustíveis) in the distillation column 10D07, which is comprised of a packing section at the bottom and plate section at the top. The packing used are Torus Saddles, a ceramic random type of packing while the plates are Montz Tunnel Trays. The reboiler (10E11) used to evaporate the mixture in the column is a vertical thermosiphon and the condenser (10E07) is an horizontal tube and shell type. The pressure implemented in this operation is close to atmospheric.

Tank 10F08 is used to collect process streams that contain methanol, water and glycerol, like the glycerol stream from the first decanter and the washing water from the crude biodiesel washing. Through the middle of the tank, fat that forms the supernatant phase is removed while, through the bottom, the aqueous phase is directed to a series of two heat exchangers where it is heated to 75°C using, in the first exchanger (10E08), the heat from the distillation column's residue stream and then steam, in the second exchanger (10E09). The already heated stream is mixed with an aqueous hydrochloridric acid stream (through static mixer 10D05) to a pH of 2.5 in order to split any residual soaps and prevent foaming in the column [29]. The column's feed is located between the packing and plate section.

In the distillation column, methanol and water are vaporized from the rest of the mixture and are continuously separated until, at the top, only methanol with less than 1000 ppm of water is obtained. The distillate from the top of the column is condensed and collected at tank 10F06. From that tank, part of the methanol then follows to the transesterification

process while the rest goes back to the column as reflux. The methanol distillate needs to have a very small amount of water since it's going to be used in the transesterification process, where the presence of water can originate hydroxyl ions which react to produce fatty acids and soaps instead of the desired methyl esters [18].

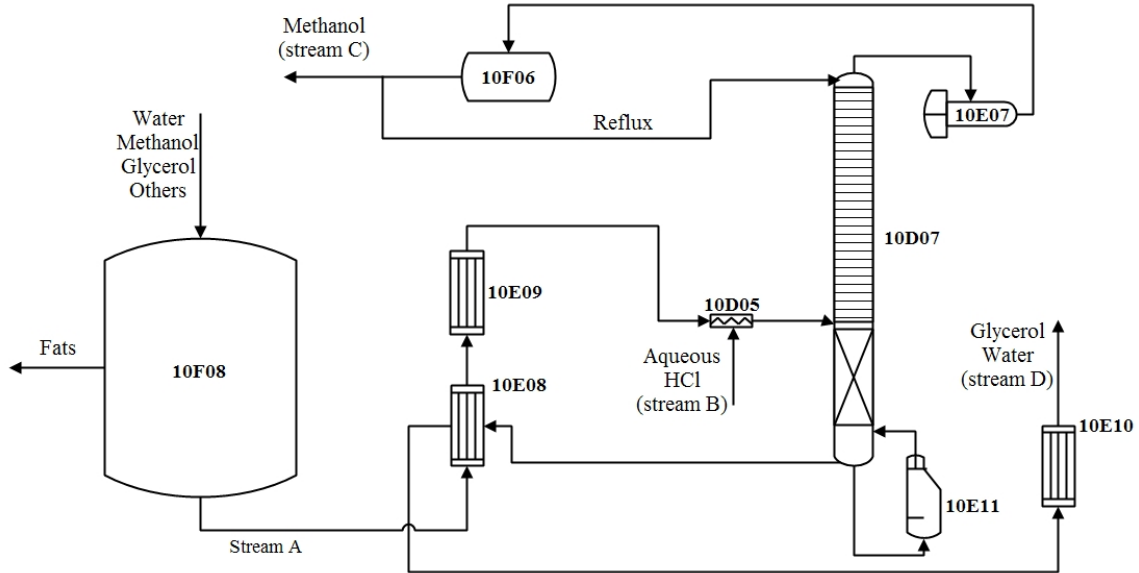


Figure 3.4: Schematic representation of the methanol recovery process at Prio Biocombustíveis S.A.

The column's residue stream, comprised of water, glycerol and a small amount of methanol and other chemicals, passes through a series of two heat exchangers (the already mentioned 10E08 and 10E10) where it's cooled before proceeding to the glycerol purification process.

Regarding the the energy requirements of the distillation column (in the form of steam provided by a boiler), this equipment is the most intensive energy consumer in the entire plant. The steam, that flows in the reboiler's shell, is used to heat the reboiler in order to create a suitable vapour flow inside the column. The heat flux transferred, by conduction, from the steam to the mixture is influenced by the thermal conductivity of the material it passes through and is given by:

$$q = -k \cdot A \cdot \frac{\Delta T}{\Delta L} \quad (3.1)$$

From equation 3.1, the inverse of $\frac{k \cdot A}{\Delta L}$ is the heat resistance of the material. In the reboiler, the heat transfer resistance comes from the reboiler's material. However, yet another resistance forms when the column is operating due to the formation of a fouling layer inside the tubes, as can be seen in figure 3.5 a and b. This fouling layer forms in the reboiler as a result of the high temperatures and presence of chemicals other than water, glycerol and methanol in the feed stream. Heat transfer equation 3.1 can be rearranged into equation

3.2, accommodating the new resistance parameter $-Re_{tot}$ - that is the sum of the fouling and reboiler resistances.

$$q = -\frac{\Delta T}{Re_{tot}} \quad (3.2)$$

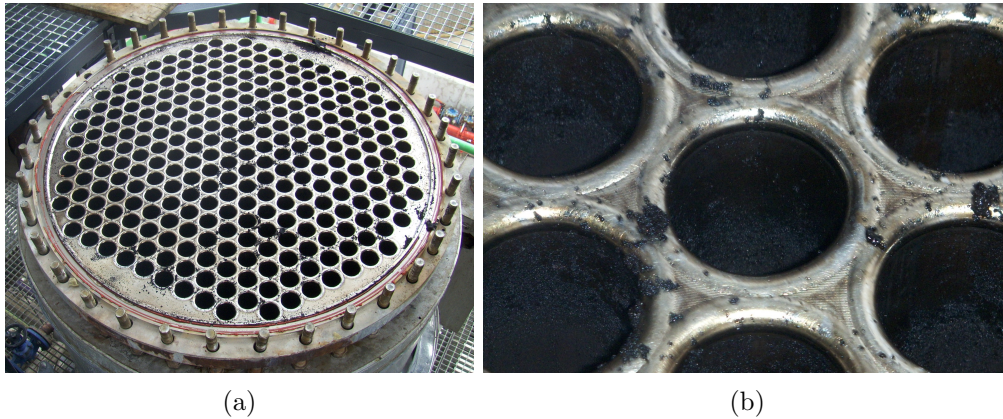


Figure 3.5: a) Distillation column's reboiler head; b) Reboiler's pipes closeup.

The existence of fouling is a main concern since, as it thickens, it increases the heat transfer resistance (as seen by equation 3.2), hindering the heat transfer from which results the use of larger quantities of steam to get the same amount of heat transferred. Understating this limitation is very important to properly manage the distillation process as well as in the search for suitable solutions for this problem.

The distillation column control is made using model predictive control (MPC) that uses both real-time measurements and a predictive model to determine the output. This specific type of control offers several advantages such as: "(1) the process model captures of the dynamic and static interactions between input, output and disturbance variables, (2) constraints on inputs and outputs are considered in a systematic manner, (3) the control calculations can be coordinated with the calculation of optimum set points, and (4) accurate model predictions can provide early warnings of potential problems" (*in Model Predictive Control* [30]). MPC is, however, only as good as the predictive model it uses and the use of an inadequate model can lead to greater instability in the process, hence the need of accurate models.

The controlled variables in the distillation process are the column's temperatures. The internal temperature profile registered corresponds to the boiling temperature of each stage's mixture, which are characteristic of each mixture's composition, thus allowing the column's temperature profile to be used as an indicative of the mixture compositions that circulate in the column. The process's manipulated variables are the reflux/feed ratio and the reboiler's steam pressure, which the MPC uses to control and lead the column's temperature profile into the desired values.

Another possible way for methanol recovery was found in the literature and is described as the dividing-wall column (DWC) [31]. It is reported that this type of equipment, when applied to the separation of methanol-water-glycerol mixtures, allows the separation of all three components while using less energy and reducing equipment costs and plant footprint, thus being an interesting alternative method to consider for new biodiesel plants or as an upgrade for already existing facilities [31].

3.1.5 Glycerol purification

Glycerol is the main by-product from oil transesterification and it can be used by other industries like the pharmaceutical or livestock food industry or as a precursor for added value chemicals like glycerol carbonate, acrolein or highly branched polymers [32, 33, 34], thus making its purification and transaction very attractive for the biodiesel industry.

The process for glycerol purification is simple, mainly due to the fact that it is only intended to upgrade the glycerol stream from a composition of 30-40% in weight to 80-90%. Sodium hydroxide is added first to set the pH to 7, following an evaporation process where water is removed until the desired glycerol composition is reached, after which the glycerol final product is obtained. A Schematic representation of the glycerol purification process at Prio Biocombustíveis S.A. is shown in figure 3.6.

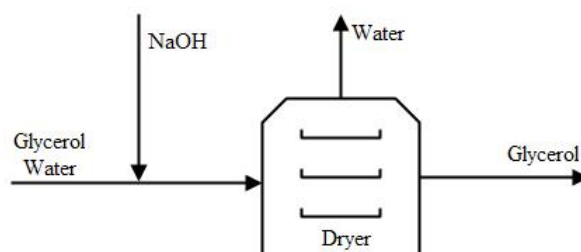


Figure 3.6: Schematic representation of the glycerol purification process at Prio Biocombustíveis S.A.

3.2 An improvement driven industry

In face of an increasingly and already very competitive fuel industry and due to the the small profit margins of the said fuels retail, raw materials price fluctuations and the existent laws and regulations (regarding both product characteristics and environmental issues), the continuous search for process performance improvements is extremely important to assure market survivability.

When a chemical plant is already installed (such as the case of Prio Biocombustíveis S.A.), this continuous improvement is many times based in updates made to the production

method, either by adding new equipments, replacing/updating dated ones for their improved versions, improving control systems or reducing waste, thus enhancing production quantity, quality and efficiency.

However, before taking any action towards improvement, one must begin by understanding and characterizing the process in question, this first step not always being easy as in many cases the information needed is not readily available or it doesn't exist at all.

As an example of common sources of information is data acquired from either the plant's control system or by the quality department. In the case of non-existent information to support decisions related to future improvements and the impossibility of getting that information directly from the process, other solutions can be applied, such as the use of simulation software or laboratory experiments.

Having acquired the data needed, the next step is its treatment to obtain useful information, statistical analysis being often the chosen path:

- The Principal Components Analysis (PCA) is a technique often applied early to identify variable's interactions.
- Design of Experiments (DoE) is another widely implemented and expeditious technique to gather experimental data according with the objective of study in that experiment. The experimental data can then be used to create empirical models.
- Multiple Linear Regression (MLR) is a technique that uses process information to generate models with more than one variable that explain the process behaviour. The type of information MLR uses can vary from experimental data to observational data.

The difference between the two data types mentioned above lies in experimental data being the product of a controlled experiment where a scientist is studying a specific parameter and intervenes in the experiment while observational data, by the contrary, is the mere observation and recording of what the scientist is observing, without his interference.

Chapter 4

Process data: stream analysis and characterization

As was mentioned in section 3.2, gathering information about the process is a crucial and initial step towards improvement as it gives a better understanding of the process, helps in detecting problems, defining process trends and in building process models. Characterization of certain key process streams is perhaps the most obvious way to obtain a detailed description of the said streams also leading to the characterization of other unanalysed streams, by means of mass and energy balances.

At the start of the present work, and since it's focus is the study of the methanol recovery process (figure 3.4), three streams were chosen to be characterised: the aqueous stream from tank 10F08 (stream A), the methanol stream from tank 10F06 (stream C) and the glycerol water stream from the bottom of the column (stream D). The selection of these streams was based on the information each could provide regarding the circulation of key components in the process and analytical methods required to do so. The samples to analyse were collected in 250 mL high density polyethylene flask.

Analytical methods used in the biodiesel industry are well established and, in most cases, regulated, by a recognized international organism or committee such as the European Committee for Standardization or the American Oil Chemists' Society. Knowing that the main components of the methanol recovery process are water, glycerol and methanol and having in mind the available laboratory equipment, the chemical analysis performed were based on the methods presented in table 4.1. It should also be mentioned that the samples collected from the base of the column had two liquid phases, the smaller and darker in color phase being the supernatant.

Table 4.1: Analytical methods used.

component	norm	method	range % (wt)
water	EN ISSO 12937:2000[35]	Karl-Fischer coulometric titration	0.003 - 0.1
	ASTM E203[36]	Karl-Fischer volumetric titration	0.1 - 100
glycerol	A.O.C.S. Ea-51[37]	Sodium Periodate oxidation	0 - 100
methanol	EN 14110[38]	Gas chromatography	0.01 - 1

4.1 Stream composition

Taking a closer look at the methanol method's range (table 4.1) and knowing, from previous experiments, that the methanol content of stream A should be in between 20-30%, it becomes obvious that this method can't be applied to this stream.

Also, it was expected that no considerable amount of glycerol would reach the top of the column, thus not contaminating the methanol recovered, due to glycerol's low vapour pressure (see appendix A). This has been confirmed by an initial analysis of the glycerol content on stream C, after which no other was made.

Still regarding stream C, as it's main contaminant is water, only this component's amount was determined for this stream, methanol comprising the remaining of the stream.

For stream D, the methanol amount was determined by gas chromatography. With methanol's mass fraction on both stream C and D, by mass balance, the mass amount of methanol in stream A was determined.

Apart from water, methanol and glycerol, other components are present in stream A and D, the second phase formed in the residue stream being evidence of this. Although these components were not identified in this work, they are likely to be methyl esters or fats from either the transesterification or methyl esters washing processes. The mass fraction of these components, from now on, called "others" in streams A and B was determined by mass balance calculations after quantifying the water, methanol and glycerol. The HCl used to acidify the column's feed is also counted in the "others" fraction.

A graphical representation of the streams compositions and reboiler's steam pressure/feed flow ratio (PV/FF) results, from 10-02-2015 to 08-04-2015, can be observed in figures 4.1, 4.3, 4.2 and 4.4. The remaining data collected during this work, regarding the column's operating conditions, can be consulted in tables B.1 to B.6 from appendix B).

Analysing figures 4.1 and 4.2, clear variations in the column's feed stream compositions can be seen, with similar variations being also registered in the column's residue stream components, except for methanol. Comparing figures 4.1 and 4.3, it becomes obvious that, although stream A suffers from significant variations, the distillate's quality is still kept, displaying a water content lower than the specified limit of 1000 water PPM.

Another important observation is that the steam pressure fed to the column's reboiler varies significantly during the column's operating period (see figure 4.4) and that higher pressures are usually accompanied by higher amounts of water at the distillate. Also, this reboiler's steam pressure increase does not result in an increase of the column's internal pressure, as seen during the start-up of the column.

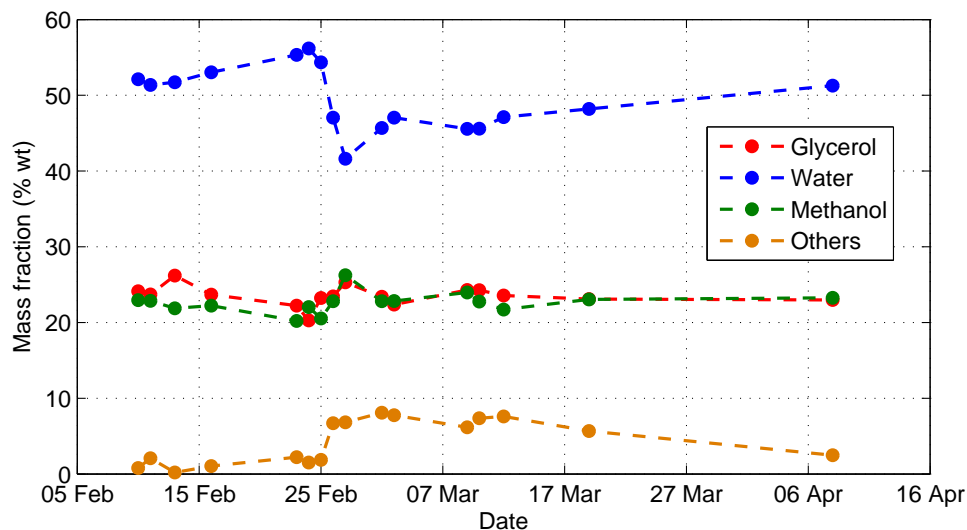


Figure 4.1: Composition of stream A in % (wt)

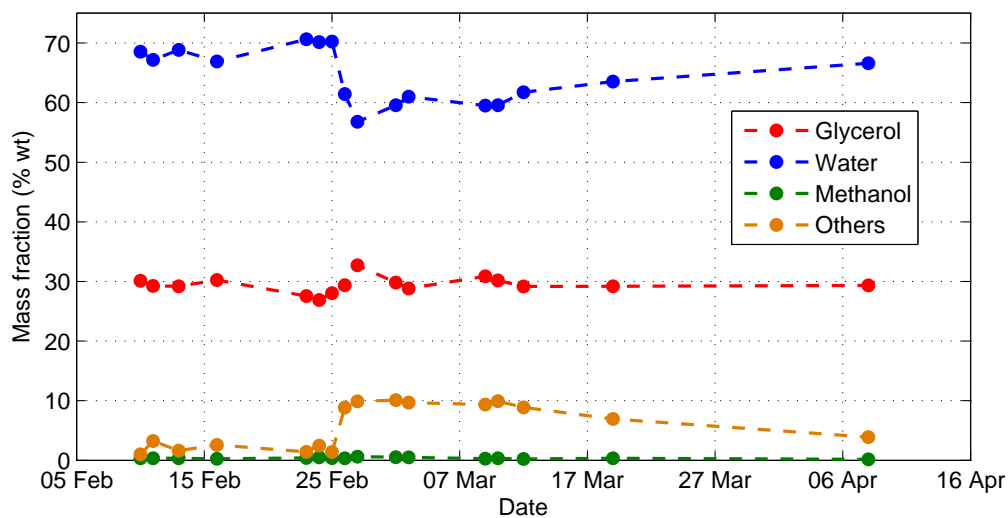


Figure 4.2: Composition of stream D in % (wt)

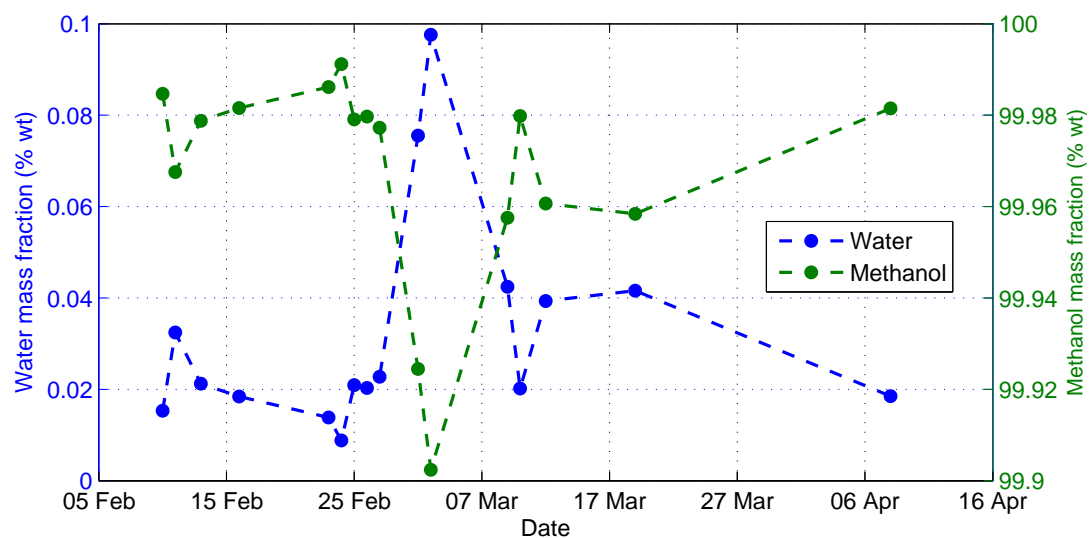


Figure 4.3: Composition of stream C in % (wt)

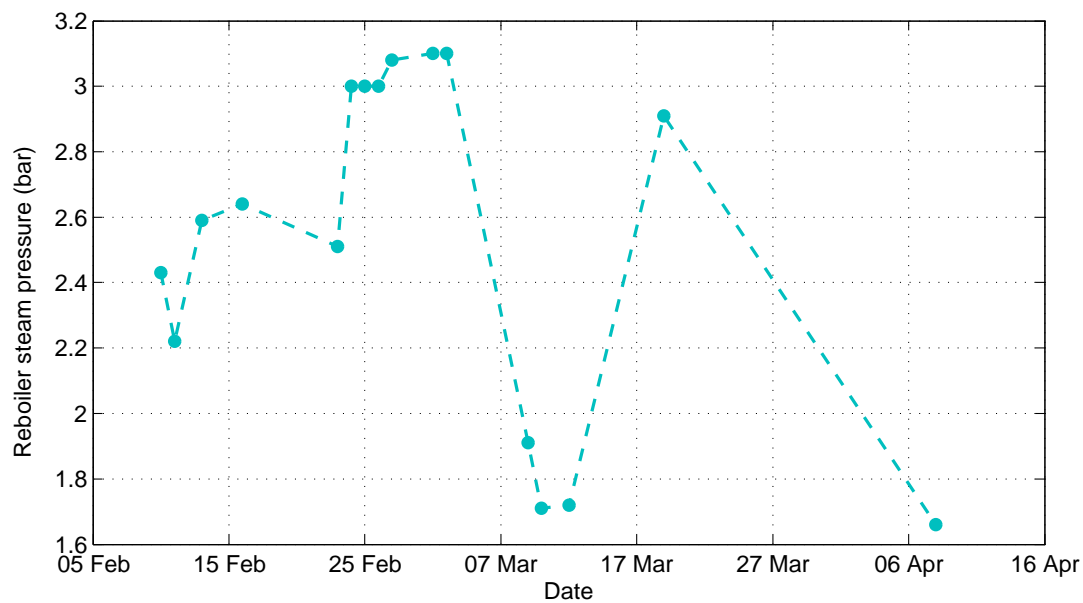


Figure 4.4: Reboiler's steam pressure variation with time.

Chapter 5

Modelling of the methanol recovery column with Aspen Plus[®]

As was mentioned before, process simulation is a powerful tool to obtain important data when it's not possible to obtain it directly from the field. In the present work, a process simulation software, namely Aspen Plus 8.6[®], was used to simulate the distillation column with the intent of evaluating the effect of certain parameters, such as components fraction in feed, reboiler outlet temperature, reflux temperature and reflux/feed ratio in the column's distillate quality.

In the previous chapter, one of the objectives in the analysis of the feed and products streams from the distillation column was to gather information that would serve as base for this simulation. However, some components were left unidentified (the ones corresponding to the "others" fraction in the streams). These components, although in small composition, are important to consider if a more accurate simulation is desired, therefore leading to the selection of 3 methyl esters to represent the "others" fraction, the three being methyl palmitate, methyl oleate and methyl linoleate. The choice of methyl esters was based in the fact that the two major streams flowing to tank 10F08 are coming from the first decanter and biodiesel washing column, where methyl esters are one of most abundant components along with water, glycerol and methanol. As for why these three in particular were chosen instead of others is due to these being the corresponding methyl esters of the most abundant fatty acids in soy, palm, rapeseed and UCO oils (see table 2.3). In the particular case of the HCl, fed to the column through stream B, it was not taken into account in the simulation due to being in small quantities and not influencing distillation. Stream B was so considered to be a simple water stream.

Having determined all components to be used, the simulation itself was kicked off with their introduction in the software. The thermodynamic model to be used was selected, in this case the UNIQUAC model with the Ideal Gas equation and using the UNIFAC parameter estimation option for the missing parameters. These are both suitable to represent liquid-

liquid and vapour-liquid equilibrium for components related with biodiesel production [39, 40].

As a result of the fouling in the reboiler, the data corresponding to the 8th of April, collected after a deep cleaning of the reboiler, was used in the simulation so that the simulation would reflect the functioning of the column at optimal conditions. In an initial stage, a DSTWU¹ model was used to estimate the number of theoretical plates needed to obtain methanol at the desired purity, this step being so important because, in the more accurate RadFrac² model, the number of stages to be used is defined by the user.

In the RadFrac model, in conformity with the real column's specifics, a lower packing section and upper plates section was set, followed by height of packing and tray number, feed composition and flow, reflux ratio, reflux temperature, distillate flow and reboiler outlet temperature. The flowsheet diagram used is represented in figure 5.1. The formation of the second liquid phase was also contemplated in the simulation.

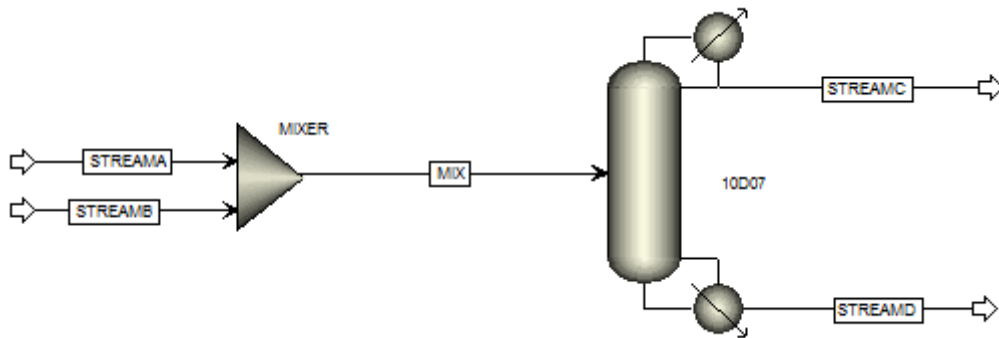


Figure 5.1: Aspen Plus® Flowsheet diagram used to simulate the distillation column with the RadFrac model.

Both the number of theoretical plates equivalent to the height of the packing and the reboiler outlet temperature were tuned until the composition of the product streams given by the simulator equalled the one determined for the samples of the 8th of April.

5.1 Thermodynamic model parameters

The choice of thermodynamic model and its respective binary interaction parameters are a factor of great influence in the accuracy of the simulation as they are the base for the equilibrium calculations.

Aspen Plus® has a very large database of binary interaction parameters that are readily available. However, some components were still not contemplated in this database having, as an alternative for this situation, the possibility to estimate the said parameters through the

¹Multicomponent shortcut distillation method.

²Multicomponent rigorous distillation method.

UNIFAC model. In the present work, parameter estimation using UNIFAC model had to be used as none of the methyl esters had its parameters in the database.

With all the required binary interaction parameters acquired, graphics with the compositions of both liquid phases, along the column, were drawn (figures 5.3 and 5.2 for the first and second phase, respectively), concluding, from their analysis, that the second liquid phase is composed of mainly FAME components while the first liquid phase contains the water, glycerol and methanol.

In the second liquid phase graphic (figure 5.2), above the 22nd distillation stage, the FAME components are no longer present and water and methanol take their place, no longer existing the second liquid phase and the first, and only, liquid phase taking its place from there on. However, some irregularities were detected as FAME components have a very low vapour pressure (see appendix A) at the column's operating conditions and shouldn't, therefore, appear above the feeding stage (stage 27). These irregularities were a sign that the binary interaction parameters used for these methyl esters were not adequate and should, therefore, be replaced by more suitable ones, these being difficult to find due to the scarcity of equilibrium data in the literature for FAME components [39].

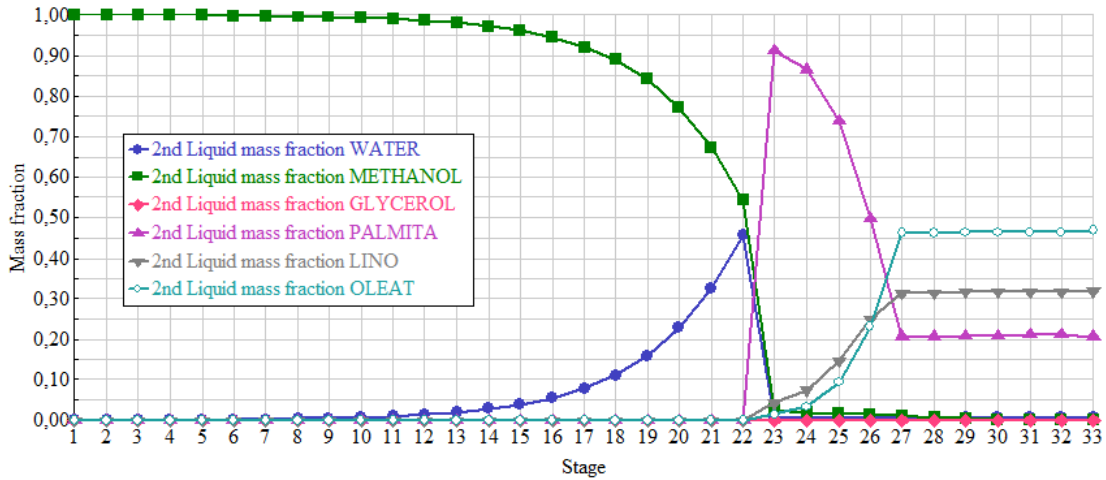


Figure 5.2: Second liquid phase composition along the column, computed with Aspen Plus®, using the software's estimated UNIQUAC binary interaction parameters.

Some of the UNIQUAC binary interaction parameters that needed to be replaced were acquired directly from the work of M. Lee *et al*[39] while others, due to the data scarcity problem mentioned before, had to be calculated using the UNIFAC model with re-estimated UNIFAC group interaction parameters specific for fatty systems, acquired from the work of G. F. Hirata *et al*[41]. The newly obtained parameters, which are presented in table 5.1, were then introduced in the simulator and the second liquid phase compositions along the column were drawn again in figure 5.4, this time not showing any unusual behaviour regarding the methyl esters. Figures 5.3 and 5.5, show the composition along the column for the liquid and

5.2. SIMULATION RESULTS

vapour phases, respectively.

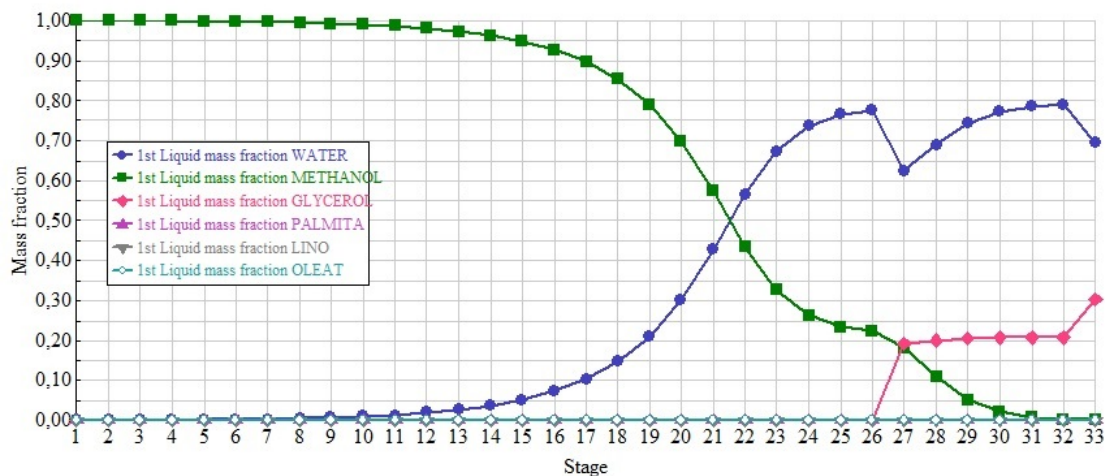


Figure 5.3: First liquid phase composition along the column, computed with Aspen Plus[®], using the software's UNIQUAC binary interaction parameters.

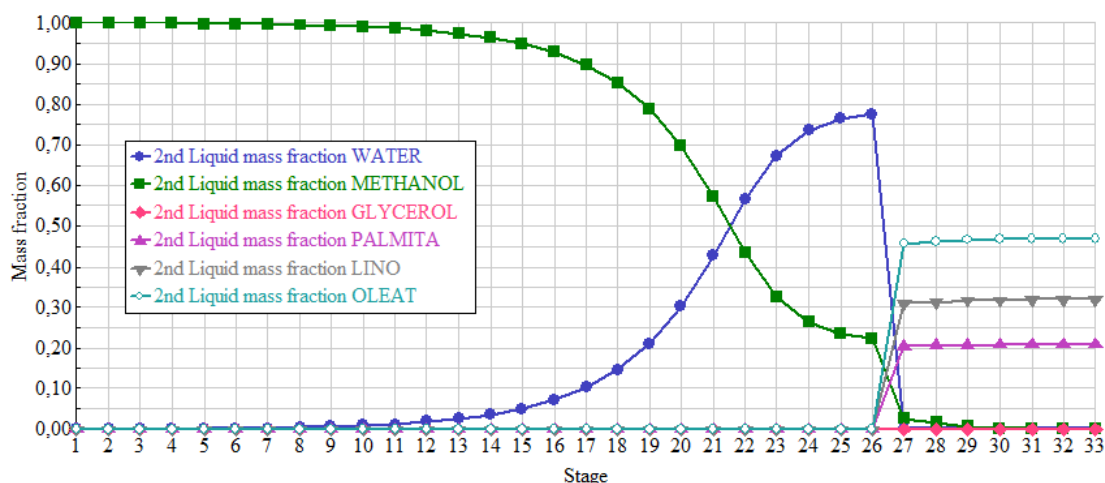


Figure 5.4: Second liquid phase composition along the column, computed with Aspen Plus[®] using the user estimated UUNIQUAC binary interaction parameters.

5.2 Simulation results

With the thermodynamic parameters now updated, the simulation proceeded without further problems and both the number of theoretical plates equivalent to the height of the packing and the reboiler outlet temperature were again tuned to obtain the product compositions observed in the samples from the 8th of April. Regarding the reboiler outlet temperature, the value that was used in the simulation was 111°C, this being in accordance with the columns operating manual that stipulated an optimum reboiler outlet temperature of about 110°C.

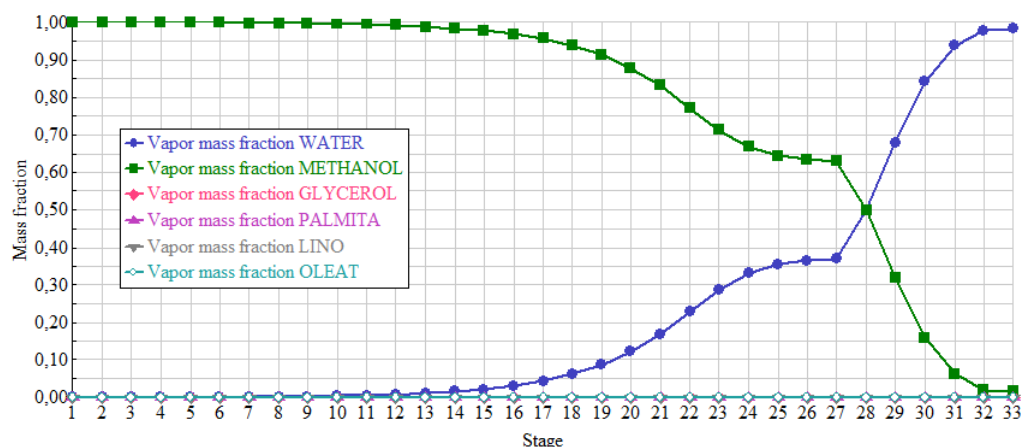


Figure 5.5: Vapour phase composition along the column, computed with Aspen Plus® using UNIQUAC parameters estimated by the user.

The results from the simulation for the 8th of April are presented in table 5.2. In the condenser, one can see that roughly 90% of the energy removed is due to the condensation of the stream and the rest due to its subcooling. Also, both reboiler and condenser heat duties are similar, this being a consequence of the energy required to vaporize the methanol and water in the reboiler being the same as the one that is extracted at the condenser. The reboiler heat duty is, however, greater since, in this equipment, apart from the the water and methanol vaporization, the remaining components are also heated to the reboiler outlet temperature. The relative error between the composition values determined by Aspen Plus® (using the standard or re-calculated UNIQUAC parameters) and the process data for the same day was also calculated and can be found in table 5.3.

A graphical representation of the temperature profiles from the simulated column, using the standard or re-calculated UNIQUAC parameter, are presented in figure 5.6. From this figure and table 5.3 analysis, it's evident that the simulator is able to replicate, relatively well, the temperature profile observed in the actual column. Furthermore, a somewhat noticeable difference in the temperature profiles can be seen between the 27th and 15th stage, this difference being a result of the different thermodynamic model parameters used, thus showing that inaccurate parameters have influence in the simulation.

The simulation was then tested using the feeding composition data from three different days and maintaining all the parameters used to simulate the column at the 8th of April. The results of these three tests are compiled in table 5.3. The larger errors for the simulation are observed for the water composition in stream C while the AARD value for the remaining components is low, this being a good indicator of the simulation's capability to represent the methanol distillation process. Part of the discrepancy seen for the water percentage in the distillate can be explained by the fact that the simulator is dealing with very small amounts and thus, even small differences in any entry parameter, such as feeding compositions, can

Table 5.1: UNIQUAC binary interaction parameters used in the simulation.

component 1	component 2	A12	A21	B12	B21
water ^a	methyl palmitate ^a	-6.6411	0.9141	2191.247	-1170.807
methanol ^a	methyl palmitate ^a	-2.6593	-4.2433	1198.464	1468.731
glycerol ^a	methyl palmitate ^a	-3.3961	-3.4759	1460.439	1109.448
methyl palmitate ^a	methyl linolate ^a	0.2547	-8.4386	43.557	3396.897
methyl palmitate ^a	methyl oleate ^a	-5.3838	-2.5133	2365.742	968.117
methyl linolate ^a	methyl oleate ^a	-4.8956	-2.2591	2159.190	860.584
water ^b	methyl linolate ^b	0	0	130.750	-1096.140
water ^b	methyl oleate ^b	0	0	120.480	-1350.700
methanol ^b	methyl linolate ^b	0	0	-97.340	-242.400
methanol ^b	methyl oleate ^b	0	0	-36.140	-280.220
glycerol ^b	methyl linolate ^b	0.9000	-50.0000	-257.950	13931.470
glycerol ^b	methyl oleate ^b	0	0	-32.050	-693.740
water ^c	methanol ^c	0.6437	-1.0662	-322.131	432.879
water ^c	glycerol ^c	0.9755	0.2609	-188.494	-45.908
methanol ^c	glycerol ^c	0	0	-100.422	-47.649

^a parameters calculated using G.F. Hirata *et al*[41] re-estimated UNIFAC parameters for the original groups.

^b parameters acquired from M. Lee *et al*[39].

^c parameters acquired from Aspen Plus® database.

introduce a large error.

With this, it can be said that the simulation can be used to simulate the behaviour of the column and to infer about the relations between its variables. The simulation shouldn't, however, be used to accurately predict the water composition on the distillate, as the error associated is large.

5.3 Sensitivity analysis

A sensitivity analysis is a method used to study how certain independent variables affect the dependant variables of a certain process, thus identifying which have a higher impact. Although the definition might be simple, implementing such a method in an industrial process is difficult as the number of variables to consider is usually large, fluctuations on those variables are common, even in continuous process, and because the disturbances created during this analysis can hinder the process, in this case the quality of the methanol recovered, later affecting the transesterification process.

However, for the sake of understanding which variables have a higher impact on the distillate purity, an alternative was found by using the simulated column in Aspen Plus® and it's local sensitivity analysis module to study how certain parameters, such as components fraction in feed, reboiler outlet temperature, reflux temperature and reflux/feed ratio, influence the process without interfering in the actual distillation column. Since this is a local variation

Table 5.2: Aspen Plus® simulation results corresponding to the 8th of April.

	composition (% wt\wt)		
	feed	distillate	residue
water	0.521	184 PPM	0.674
methanol	0.229	1	0.002
glycerol	0.226	TR	0.292
methyl palmitate	0.005	TR	0.007
methyl linoleate	0.008	TR	0.01
methyl oleate	0.012	TR	0,015

	condenser	reboiler
inlet temperature (°C)	65.2	105
heat duty (kW)	-918.9	1099.7
subcooled duty	-95.2	-
outlet temperature	29.4	111

analysis, the variation range considered for each variable was set having in consideration the limit operating conditions for the actual column.

To make this analysis easier, the absolute values obtained were converted to percentage increments or decrements, with the original simulation results corresponding to 0%. These percentages were determined according to equation 5.1:

$$\% = \frac{\Xi_{i,1} - \Xi_{i,0}}{\Xi_{i,0}} \times 100 \quad (5.1)$$

here $\Xi_{i,1}$ represents the variable's new value and $\Xi_{i,0}$ the original variable's value. The results from this analysis were then converted to graphics, those being presented in figures 5.7 to 5.12. As this analysis is being made to understand which variables significantly affect the distillate purity, variations of -0.082% or lower in the purity will not be taken into consideration as they don't give rise to out of specification distillate. The reason as to why such a slight change in the distillate quality is considered significant is mainly due to the fact that the distillate purity required is extremely high (< 1000 PPM of water), thus making variations of -0.082% , and lower, relevant to the methanol distillate mass fraction.

Figure 5.7 shows the increase, in percentage, of the methanol mass fraction at the distillate with the increase of the reflux/feed ratio. It is evident that, for the reflux/feed ratio variation range considered, the lower limit at which the distillate purity was overcome was for -4% and lower variations. As for positive variations of the reflux/feed, no perceptible changes in the quality of the distillate are seen, its value being already higher than the required distillate purity.

Figure 5.8 depicts the decrease, in percentage, of the methanol mass fraction with the increasing reboiler outlet temperature. Regarding the overall methanol mass fraction vari-

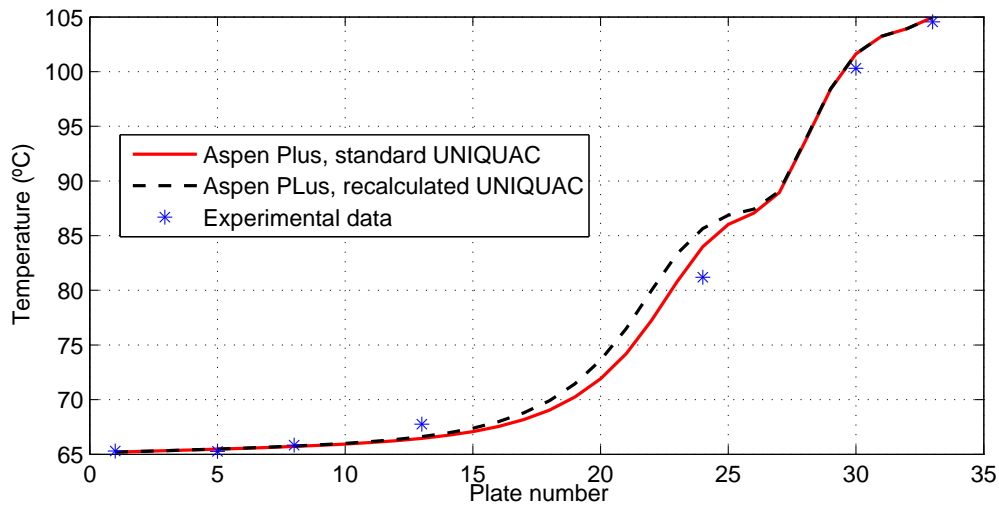


Figure 5.6: Distillation column's temperature profiles.

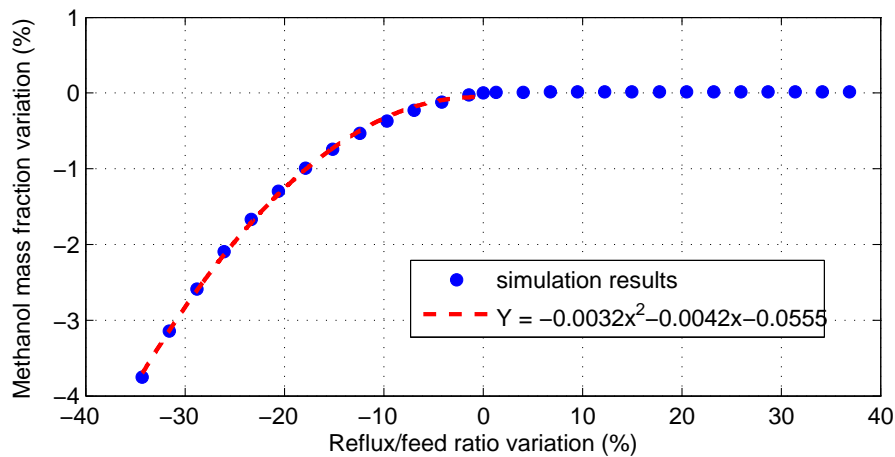


Figure 5.7: Variation of the methanol mass fraction at the distillate with the variation of the reflux/feed ration.

ation seen in this figure, it can be seen that the lowest value observed is still far from the limit at which the distillate is out of specification with the addition that, for higher reboiler outlet temperature variations, the variation in the distillate tends to a constant value close to -0.02% . It should also be mentioned that reboiler outlet temperature variations lower than -2% are not considered since a temperatures lower than that is not compatible with the column's operation as it is not high enough for the mixture to start boiling.

Figure 5.9 is referent to the decrease, in percentage, of the distillate methanol mass fraction with the increase in reflux temperature. As can be seen, the variation in the distillate hasn't reached the limit at which it it out of specification. However, considering the behaviour of the curve, as the reflux temperature variation increases it is expected that the distillate quality will also decrease.

Table 5.3: Comparison between the Aspen Plus® given compositions and the compositions observed in the field (% wt/wt) for streams C and D.

		residue				distillate	
		simulation setting					
		glycerol	water	methanol	“others”	water	methanol
08-04-2015 ^a	observed	29.33	66.61	0.18	3.88	0.02	99.98
	Aspen Plus	29.25	67.41	0.17	3.16	0.01	99.99
	AARD (%)	0.29	1.21	2.13	18.46	22.86	<0.00
08-04-2015 ^b	observed	29.33	66.61	0.18	3.88	0.02	99.98
	Aspen Plus	29.25	67.41	0.18	3.16	0.02	99.98
	AARD (%)	0.29	1.20	1.44	18.46	0.31	<0.00
		simulation testing					
09-03-2015	observed	30.87	59.49	0.29	9.35	0.04	99.96
	Aspen	31.18	60.63	0.28	7.90	0.02	99.98
	AARD (%)	1.03	1.92	4.79	15.50	60.06	0.03
02-03-2015	observed	29.81	59.55	0.53	10.11	0.08	99.92
	Aspen	29.54	59.73	0.50	10.22	0.01	99.99
	AARD (%)	0.90	0.30	5.51	1.16	85.26	0.06
12-03-2015	observed	29.18	61.74	0.22	8.87	0.04	99.96
	Aspen	29.41	60.90	0.21	9.48	0.01	99.99
	AARD (%)	0.82	1.36	3.37	6.86	70.53	-0.03

^a results for the simulation prior UNIQUAC parameters correction.

^b results for the simulation after UNIQUAC parameters correction.

At last, figures 5.10, 5.11 and 5.12 are about the variation of the methanol mass fraction at the distillate by varying the amount of the 3 main components of the column’s feed: water, methanol and glycerol. Starting with the water variation (figure 5.10), as it increases, distillate purity decreases. In turn, when the methanol amount at the feed increases, the distillate purity also increases. As for the glycerol, as it increases, almost no variation in the distillate occurs.

With all the graphics drawn, a common feature can be seen in all of them, except in the one regarding glycerol, it being that, at some point, the impact on the methanol mass fraction variation would tend to a stable value, thus enabling the identification of two different operating zones: the first being an area where significant variations could be seen and the distillate is out of specification and the second being an area where no significant changes can be seen and the distillate is within the specified requirements. With this, and considering that the objective of this test was to determine how much each variable affects the methanol recovery process, a second degree equation for figures 5.7 to 5.12 was adjusted to the data in the operating zone with significant variations. Those equations were then derived to obtain the methanol mass fraction sensitivity to change with each variable tested and to establish an order of importance, based on these derivatives, for the tested variables, which can be seen in table 5.4. The variables are ordered decreasingly, in the table, regarding its impact.

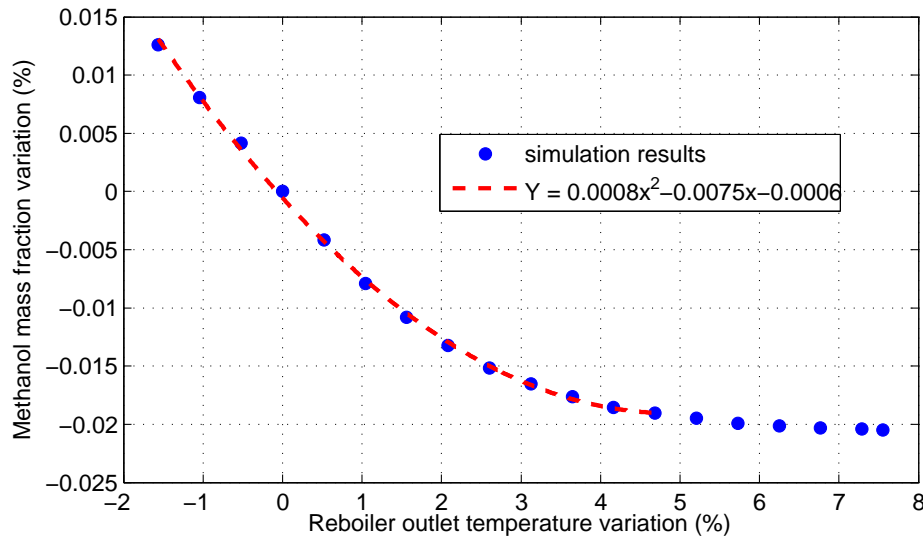


Figure 5.8: Variation of the methanol mass fraction at the distillate with the variation of the reboiler outlet temperature.

From the sensitivity analysis comes that the variable with the highest impact in the process is the methanol on feed, followed by the reflux/feed ratio, reflux temperature, water on feed, reboiler outlet temperature and, lastly, the glycerol on feed.

Apart from being able to arrange the tested variables by their degree of impact in the process, this test also enabled a larger understanding of what happens when one of the said variables is affected by a variation:

- When there is a methanol decrease on the feed stream, as there is less methanol entering the column, if the distillate flow is not adjusted to the current value of inlet methanol, what happens is that water will be recovered along with methanol in the distillate. This situation can be avoided by controlling the distillate flow to be the same (or very similar) as the methanol amount fed to the column. A similar situation can occur when the total feed flow varies, also requiring an adjustment to the distillate flow.
- As the amount of water in the feed increases, so do the process requirements, leading to the decrease in the distillate quality. As a countermeasure for this, an increase of reflux/feed ratio can be made to move the distillate back to the desired specifications.
- Regarding the reflux/feed ratio and the reflux temperature, the existence of a zone, in the corresponding graphics, in which the variation of the distillate's purity tends to a constant value can be interpreted as the optimal limits of operation, but only for this particular feed composition, existing other optimal limits for different feed compositions.

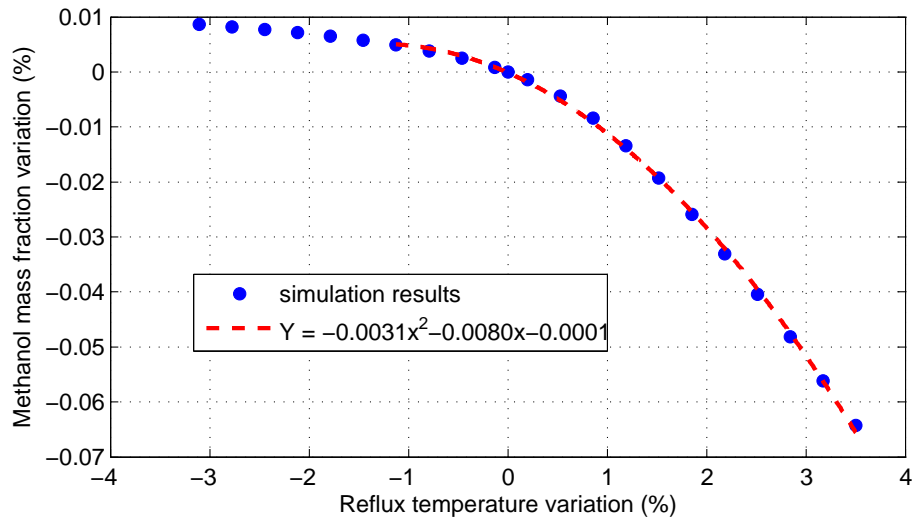


Figure 5.9: Variation of the methanol mass fraction at the distillate with the variation of the reflux temperature.

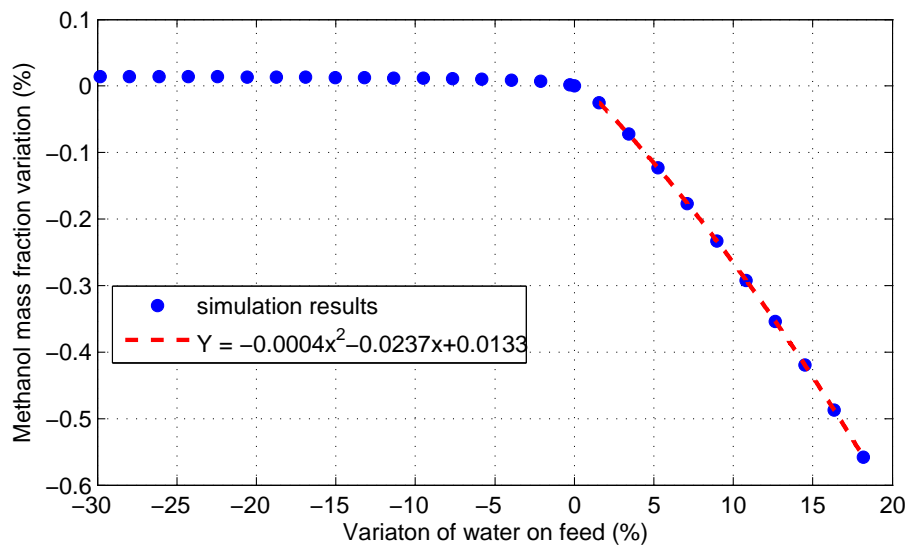


Figure 5.10: Variation of the methanol mass fraction at the distillate with the variation of water amount in the feed stream.

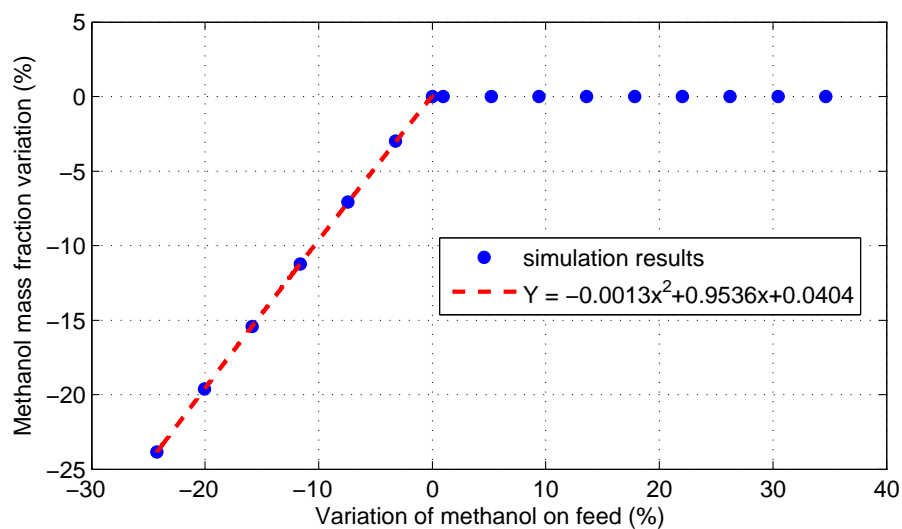


Figure 5.11: Variation of the methanol mass fraction at the distillate with the variation of the methanol amount in the feed stream.

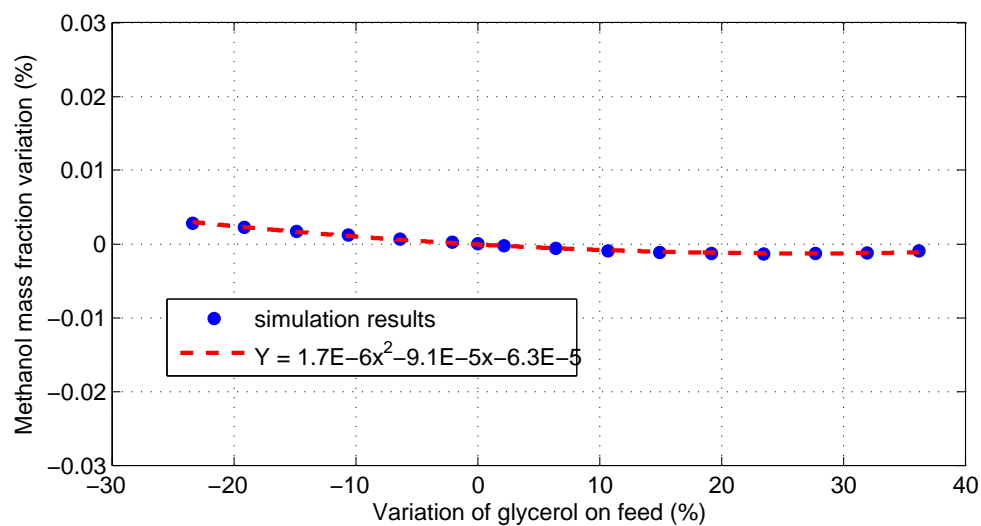


Figure 5.12: Variation of the methanol mass fraction at the distillate with the variation of the glycerol amount in the feed stream.

Table 5.4: Equations, and respective derivatives, from the fitted data for each variable in study.

	variable, x	equation	derivative
	methanol		
1	on feed	$Y = -0,0013x^2 + 0,9536x + 0,0404$	$Y' = -0,0026x + 0,9536$
	reflux/feed		
2	ratio	$Y = -0,0032x^2 - 0,0042x - 0,0555$	$Y' = -0,0064x - 0,0042$
	reflux		
3	temperature	$Y = -0,0031x^2 - 0,0080x - 0,0001$	$Y' = -0,0062x - 0,0080$
	water		
4	on feed	$Y = -0,0004x^2 - 0,0237x + 0,0133$	$Y' = -0,0008x - 0,0237$
	reboiler outlet		
5	temperature	$Y = 0,0008x^2 - 0,0075x - 0,0006$	$Y' = 0,0016x - 0,0075$
	glycerol		
6	on feed	$Y = 1,7 \times 10^{-6}x^2 - 9,1 \times 10^{-5}x - 6,3 \times 10^{-5}$	$Y' = 3,4 \times 10^{-6}x - 9,1 \times 10^{-5}$

Y is the is methanol mass fraction variation in the distillate.

Chapter 6

Methanol recovery process models

Process data from the distillation process is, as was said in chapter 4, a most valuable resource when studying a process. Not only it allows to directly evaluate the column's performance, by comparing those values with process references, but it can also be used to study the relationships between certain parameters or even to construct mathematical models used to estimate process outputs.

This chapter deals with the analysis of process data using statistical methods such as the Principal Components analysis (PCA) and the Multiple Linear Regression method (MLR). Apart from the data collected during this work, production history data from the company was also used. The Design of Experiments (DoE) was also implemented with the objective of gathering experimental data.

6.1 PCA

The Principal Components Analysis is a method used to reduce the data's dimensionality of a large number of interrelated variables, by transforming them into a smaller number of Principal Components (PC), whilst retaining as much of the original variable's variation as possible. PCA's importance and role as a method to assess variable's relations is also enormous, making it an important tool in the study of complex processes [42].

The PCs resulting from the analysis are ordered by decreasing eigenvalue. The cumulative variability is another important result as it tells how much of the variability of the data is represented by the number of PCs.

Resorting to Minitab 17[®] statistical tools, a Principal Components analysis was made with data from the distillation process. The data was normalized prior Principal Components Analysis due to different variables with different units and variations being present, which could mean that, if not normalised, the variables with the larger variance would tend to dominate the first PCs, producing masqueraded results [42]. The results for the distillation process's PCA are presented in table 6.1. For this analysis, neither glycerol nor "others"

related variables were considered, since their data was incomplete, and the names of the variables used are presented in table 6.2.

Table 6.1: Eigenvalue and commutative variability for the methanol distillation process PCA.

	PC1	PC2	PC3	PC4	PC5	PC6
Eigenvalue	5.475	4.424	2.047	1.655	1.031	0.990
Cumulative	31.5	57.0	68.8	78.4	84.3	90.0
	PC7	PC8	PC9	PC10	PC11	PC12
Eigenvalue	0.524	0.339	0.299	0.185	0.148	0.108
Cumulative	93.0	95.0	96.7	97.8	98.6	99.3
	PC13	PC14	PC15	PC16	PC17	
Eigenvalue	0.061	0.031	0.025	0.012	0.000	
Cumulative	99.6	99.8	99.9	100.0	100.0	

There is no universal rule to determine the number of PCs to use and, in each case, a careful assessment of the problem in study should be made in order to provide some insight to guide in this matter. One of the most widely used criteria is the cumulative variability and normal cut-off values of between 70-90% are commonly used. However, in some cases, smaller or higher cut-off values can be used like, for example, when one or two PCs are the obvious responsible for the majority of the variation, a cut-off value higher than 90% might be needed get information on the less obvious structures. The opposite example is when a large number of variables is present and a cut-off of 70% might still represent a large number of PCs to analyse, thus requiring a somewhat lower cut-off to diminish that number [42].

For the present Principal Component Analysis, the cumulative variability cut-off will be the criteria used and, although the number of variables is not that large, it was decided that a somewhat close to the normal lower limit cut-off would be used as to keep PC analysis simple. The cut-off value was set at 75% and the lowest number of PCs that had a cumulated variability higher than that was four, representing a total cumulative variability of 78.4%. In table 6.2, the PC's coefficients for the first four PCs are presented.

The PC coefficient's are attributed to each variable and, together, they represent the variation of said PC. Coefficient's values can range from zero to +/-one: values close to zero means that that certain variable is responsible for almost no variation in that PC while values close to one indicate high variable influence.

The loadings plot is a representation of the vector of coefficients and is very useful in interpreting the results as it gives a visual representation of the variables relations and importance, helping with the interpretation of the PC coefficients . The loadings plot for the first three PC's is presented in figure 6.1.

Analysing the coefficients for each PC in table 6.2, a cut-off value of 0.3 was considered and the variables whose coefficients were above that value are regarded as the ones translating

Table 6.2: Principal Components coefficients for the variables of the methanol recovery process.

initials	variable	PC1	PC2	PC3	PC4
WF	water at feed	-0.261	0.197	-0.303	0.367
WB	water at residue	-0.232	0.141	-0.375	0.407
WT	watter at distillate	0.315	0.254	-0.188	-0.015
MF	methanol at feed	0.265	-0.236	0.216	-0.125
MB	methanol at residue	-0.103	0.367	0.317	-0.057
MT	methanol at destillate	-0.315	-0.254	0.188	0.015
FF	feed flow	-0.054	-0.265	0.230	0.246
R	reflux/feed	-0.046	-0.419	0.006	0.18
T3	T102403	0.179	-0.161	0.199	0.231
T4	T102404	0.378	-0.098	0.055	0.212
T5	T102405	0.385	0.043	-0.003	0.138
T6	T102406	0.382	0.105	-0.185	0.135
T7	T102407	0.253	-0.240	-0.353	0.058
T8	T102408	-0.111	-0.238	-0.463	-0.159
T9	T102409	0.075	-0.348	-0.209	-0.206
PI	internal pressure	-0.105	-0.227	0.138	0.516
PV	steam pressure	0.176	0.203	0.133	0.339

the larger variability in the said PC, them being highlighted at bold in the table: for the first PC they are water at distillate, methanol at distillate and thermocouples T102404, T102405 and T102406 temperatures; for the second PC they are methanol at residue, reflux/feed ratio and thermocouple T102409 temperatures; for the third PC they are water at residue, methanol at residue and thermocouples T102407 and T102408 temperatures; for the fourth and final PC they are water at feed and residue, column's internal pressure and reboiler's steam pressure.

Paying now closer attention to these variables, the following relations can be withdraw:

- Thermocouple T102404, T102405 and T102406 coefficients are close to each other, showing a relation between the three as they represent the temperature corresponding to the rectification section of the column. Thermocouple T102403 temperature is not included in this group because it registers the value of temperature at the column's first plate, in which barely no separation occurs, therefore showing low variation too, this plate being instead used as an indicative of the distillate's quality.
- The water at distillate and methanol at distillate also show an already expected symmetry since they both represent the distillate's purity, one being determined from the other.
- Thermocouple T102409 and methanol at residue can be related through both mixture boiling point and reboiler heat: as the reboiler heat increases, more methanol is evapo-

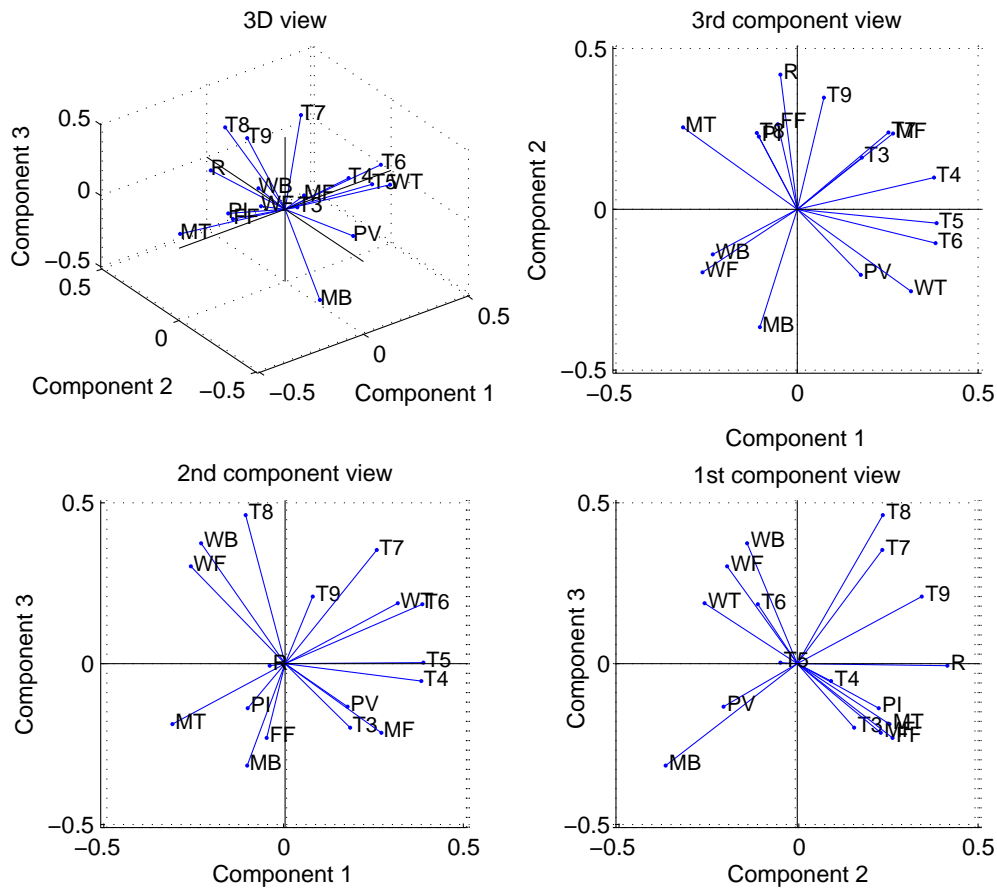


Figure 6.1: Loadings plot of the variables in the methanol distillation process PCA for the first three PCs.

rated leading to a lower fraction of this component at the residue which, consequently, results in a higher mixture boiling point, which is given by T102409.

- Reflux/feed ratio, feed flow and column's internal pressure are also related with each other. The relation between the reflux/feed ratio and feed flow is pretty straightforward since the feed flow is used to calculate the reflux/feed ratio. As for the relation with internal pressure, as the reflux/feed ratio increases, so does the column's internal vapour phase and consequently the internal pressure.
- The water at feed and residue is another already expected relation since practically all the water that enters the column exits through the residue. Therefore, when water varies at feed so it does at the residue, this being easily demonstrated by the column's water mass balance.
- It is known that the already above mentioned reboiler heat is related with the steam pressure fed to the reboiler. It is also known that the more heat transferred, the more

water and and methanol evaporated and the higher the internal pressure. However, although the reboiler's steam pressure does vary, the PCA gives no clear relation between the steam pressure and column's internal pressure. An explanation for this comes from the fouling in the reboiler. As fouling sets, the heat transfer diminishes and a higher amount of steam is required to keep the heat transferred constant thus, although a variation in the steam pressure exists, no related variation in the internal pressure is seen since the heat available to evaporate the water and methanol remains the same.

Based on chapter's 5 sensitivity analysis and this chapter's PCA, although the distillation processes is, in theory, easy to understand, the complexity of Prio Biocombustíveis S.A. methanol distillation process is not small as there are many variables that affect the process and a large number of interactions between those variables, making it a demanding process to manage.

6.2 Distillate purity

Models for estimating process outputs are very important in process management as they can give a fast assessment on the process status. Such models can either be empirical or mechanistic, the empirical methods being based on empirical data while mechanistic models require deep knowledge of the process variables interactions to construct the model. Although these models are usually more accurate and provide a deeper understanding of the interactions between the dependant and independent variables than empirical models, their complexity is also higher making them harder to obtain.

Considering the above, and having easy access to process data, and the sensitivity curve values obtained from the simulator Aspen Plus, as described in the previous chapter, it was chosen to build an empirical model to estimate the distillate's purity (dependent variable). As for the independent variables to be used in the model, both reflux/feed ratio and T102407 thermocouple temperature were selected since they are controlled variables in the process, thus being possible to vary them at will. The use of these variables is also advantageous since they are continuously measured on-line, making them readily available and updated.

The objective of the distillate's purity model is to provide an estimate of the amount of water present in the methanol distillate, allowing its constant monitoring without the need to collect and analyse distillate samples, saving both time and resources in the process. Apart from this, such an equation can also be used to provide set-points for either reflux/feed ratio or T102407 that will correspond to a desired distillate purity.

To create the above mentioned model, the Multiple Linear Regression method was used with process data, either experimental (obtained from a Design of experiments) or observational (acquired by collecting samples and information on the process).

6.2.1 Design of Experiments

The Design of Experiments (DoE) is a method used to investigate how certain input variable changes affect the output variables by performing a series of runs in which the desired input variables are subjected to a predefined variation while keeping the other variables constant [43, 44]. The number of runs required for this method depends on the factors to be studied (variables) and the levels for each factor (number of values to be tested) and is given by $n = \text{factor}^{\text{variable}}$. This method, when successfully implemented, can provide experimental data that is representative of the factors in study while, at the same time, being a lot less time consuming and exhaustive than one-factor-at-a-time experiments [44].

Given the DoE's advantages, a 2^2 level factorial design of experiments was attempted in order to study the effect of the reflux/feed ratio and thermocouple's T102407 temperature on the distillate's water and to obtain an empirical model to estimated the distillate's purity. Between each DoE run, a period of around 3 hours was given for the column to reach the stationary state for the desired conditions.

The DoE's runs were carried out till completion, its results being displayed in table 6.3, in which is visible that, for the design temperature of 79°C , the true value recorded for both runs at this temperature was not the same, existing a 1°C difference between them, thus rendering this DoE inconclusive as the variation seen in the water at distillate might be influenced by that temperature difference. Also, during the time of the experiment, feed stream compositions changed slightly (see column feed compositions for the 10th of March in table of B.1, apendix B), this too being another reason to discard this DoE. The difference in temperatures is given to the instability in the column when the set point for T102407 was changed from 82°C to 79°C , which made impossible for the temperature to stabilize during the experiment.

Table 6.3: Water on distillate results for the 2^2 factorial design of experiment for T102407 temperatures of 79°C and 82°C and for reflux/feed ratios of 33 and 37. $T_{7,\text{obs}}$ and R/FF_{obs} represent the true values of T102407 and reflux/feed registered during the experiment.

		reflux/feed ratio	
		33	37
T102407 $^\circ\text{C}$	79	202PPM	167PPM
		$T_{7,\text{obs}}=79.2$	$T_{7,\text{obs}}=78.2$
		$R/FF_{\text{obs}}=32.8$	$R/FF_{\text{obs}}=36.9$
	82	536PPM	393PPM
		$T_{7,\text{obs}}=82.0$	$T_{7,\text{obs}}=82.0$
		$R/FF_{\text{obs}}=32.8$	$R/FF_{\text{obs}}=37.0$

Given the first DoE's failure, a second attempt was made, this time being a 3^2 level factorial design and paying special attention to the DoE's planning in order to prevent temperature oscillations in the column as much as possible by making small, step-by-step, variations in-

stead of an abrupt change in the desired variable as well as taking two samples at each pair of temperature and reflux/feed ratio. However, regardless of previous preparations, this experiment was not carried out past the first temperature (78°C), as seen in table 6.4) because, just like in the first case, not only temperature oscillations started to occur during the temperature set-point variation from 78°C to 80°C but, again, because the column's feed steam composition changed (see column feed compositions for the 3rd of June in table of B.1, appendix B).

Table 6.4: Water on distillate results for the 3^2 factorial design of experiment for T102407 temperatures of 78°C, 80°C and 82°C and for reflux/feed ratios of 0.32, 0.34 and 0.36. $T_{7,obs}$ and R/FF_{obs} represent the true values of T102407 and reflux/feed registered during the experiment.

T102407 (°C)	reflux/feed ratio			
	32		34	
	1	2	1	2
	270PPM	228PPM	173PPM	167PPM
	($T_{7,obs}=78.2$ $R/FF_{obs}=0.319$)	($T_{7,obs}=78.1$ $R/FF_{obs}=0.319$)	($T_{7,obs}=77.8$ $R/FF_{obs}=0.34$)	($T_{7,obs}=78.0$ $R/FF_{obs}=0.340$)
78				
80	-	-	-	-
82	-	-	-	-

T102407 (°C)	reflux/feed ratio	
	36	
	1	2
	119PPM	160PPM
	($T_{7,obs}=76.9$ $R/FF_{obs}=0.359$)	($T_{7,obs}=76.8$ $R/FF_{obs}=0.360$)
78		
80	-	-
82	-	-

Although the prepared DoE's failed to produce the experimental results needed to create a distillate purity model based in statistically designed experiments, other conclusions can be withdrawn, regarding the behaviour of the column when the set-point of T102407 changes: there is a delay between the moment the set-point is changed and a response in T102407 is observed (process delay time), thus giving birth to temperature oscillations which grow larger the larger the initial disturbance in set-point. It can also be seen that, as the reflux/feed ratio increases, T102407 temperature diminishes.

6.2.2 Multiple Linear Regression

Having failed to acquire experimental data from statistically designed experiments, observational data, collected during the present work, was used instead.

The widely used multiple Linear Regression method (MLR) adjusts a linear equation with more than one variable regressor to a set of empirical data[45]. The multiple linear regression

model obtained to describe the data is presented as an equation of the type:

$$y = \beta_1 + \beta_2 v_1 + \beta_3 v_2 + \dots \beta_k v_k + \varepsilon \quad (6.1)$$

For more complex models, like equation 6.2, containing interaction or crossed parameters such as $v_k \times v_i$ or $v_k \times v_k$, the MLR method can still be employed by transforming the higher order arguments into new variables, as can be seen in equation 6.3 [45].

$$y = \beta_1 + \beta_2 v_1 + \beta_3 v_2 + \beta_4 v_1 \times v_2 + \beta_5 v_1 \times v_1 + \varepsilon \quad (6.2)$$

$$y = \beta_1 + \beta_2 v_1 + \beta_3 v_2 + \beta_4 v_3 + \beta_5 v_4 + \varepsilon, \quad v_3 = v_1 \times v_2 \text{ and } v_4 = v_1 \times v_1 \quad (6.3)$$

MLR, although being a powerful and easy to apply tool has its limitations. In general, empirical model's validity can only be guaranteed within the regressing variables range[45]. Also, when the data collected belongs to a controlled process, such as in this work, the regressing variable's variations is limited by the process control which might lead to important information, outside of the allowed regressing variables range, to be lost [45]. It should also be mentioned that this method is highly dependent of the amount and quality of the data upon which the regression is being made.

To build the MLR model, a stepwise algorithm, following a bidirectional approach, was used to add and/or remove parameters. With the collected data corresponding to the reflux/feed ratio, thermocouple T102407 temperature and water mass fraction in the distillate and resorting to Minitab 17[®] regression tool, an initial regression was created with only first order parameters, following the addition and/or removal of new parameters. When the latest regression parameters *P-value*¹ hit 0.05 or higher, the algorithm would stop and the previous regression with the higher coefficient of determination (R^2) would be chosen. The regressions obtained up to the stooping criteria was verified are presented in table 6.5. As can be seen in the table, only the first order regression and the first order regression with $v_1 v_2$ term show *P-values* lower than 0.05. However, when looking at their low coefficient of determination and high absolute average relative deviations, both regressions were discarded since the estimation of water on distillate with these models was no where near being trustworthy.

Given the inefficacy of the previous regressions to estimate the amount of water in the distillate, another attempt was made using the same algorithm as before but changing thermocouple T102407 temperature with thermocouple T102405, as the second regressing variable, and keeping the reflux/feed ration as the first regressing variable. This change was made based on the results from the Principal Components Analysis which indicated both variables

¹The *P-value* is used to to determine statistical significance in a hypothesis test. It evaluates how well the tested data supports the null hypothesis. For high *P-values*, the null hypothesis is considered true and vice-versa. In the present work, when the *P-value* is lower than 0.05, the null hypothesis is not considered.

Table 6.5: MLR results for the water on distillate model, using reflux/feed ratio and thermocouple's temperature T102407.

	1° order		1° order + v_1v_2 interaction		2° order	
R^2	0.533		0.604		0.539	
$AARD$ (%)	347.25		369.12		60.95	
term	P -value	coef.	P -value	coef.	P -value	coef.
constant	0.004	-2917	0.006	-39998	0.559	30929
reflux/feed	0.000	-5889	0.015	104943	0.993	-212
T102407	0.000	65.3	0.004	538	0.546	-816
reflux/feed ²	-	-	-	-	0.816	-8878
T102407 ²	-	-	-	-	0.514	5.58
reflux/feed × T102407	-	-	0.011	-1413	-	-

as being the most influential variables in the first and second PCs. The newly obtained regressions are presented in table 6.6.

From the regressions made with the reflux/feed ratio and T102405, the one that exhibits a P -values higher than 0,05 is the second order regression with the interaction parameter. From the remaining three regressions, the one corresponding to the first order with the v_1v_2 interaction parameter exhibits the highest R^2 value of 92.93% as well as the lowest value of $AARD$ of 19.44% and was, therefore, selected to be used as a model to estimate the water amount on the distillate (equation 6.4).

$$\begin{aligned}
 x_{wtr,top}(PPM) = & -208612 + 558780 \times \text{reflux/feed} + 3188 \times \text{T102405} \\
 & - 8533 \times \text{reflux/feed} \times \text{T102405} \quad (6.4)
 \end{aligned}$$

The relatively high $AARD$ of equation 6.4 can be seen as a consequence of using only two variables to estimate the water on distillate. As was seen on the PCA, even though the reflux/feed and T102405 are the most influential variables in the first and second PCs, they are still insufficient to represent the majority of the process variability. This model, however, even with an $AARD$ of 19.44, can still be considered good and simple enough to be used to get a rough estimate of the distillate's quality and to assess the distillation process performance without requiring any chemical analysis.

It should also be mentioned that what is tried to model here is a residual water concentration on the distillate which is very susceptible to small variations on either one of the model's variables. Considering the normal variation seen in the on-line measurement of both reflux/feed and thermocouple T102405 temperature, part of the model's error can be explained by it.

Since the initial objective was to create a model that included thermocouple T102407

Table 6.6: MLR results for the water on distillate model, using reflux/feed ratio and thermocouple's temperature T102405.

	1° order		1° order + v_1v_2 interaction	
R^2	0.87		0.93	
$AARD$ (%)	22.55		19.44	
term	P-value	coef.	P-value	coef.
constant	0.00	-27284	0.00	-208612
reflux/feed	0.00	-3148	0.00	558780
T102405	0.00	434	0.00	3188
reflux/feed ²	-	-	-	-
T102405 ²	-	-	-	-
reflux/feed × T102407	-	-	0.00	-8533
	2° order		2° order + v_1v_2 interaction	
R^2	0.90		0.94	
$AARD$ (%)	33.60		90.98	
term	P-value	coef.	P-value	coef.
constant	0.003	664717.0	0.371	182893
reflux/feed	0.025	-26838.0	0.000	454129
T102405	0.002	-20369.0	0.171	-8139
reflux/feed ²	0.047	36157.0	0.250	17617
T102405 ²	0.002	157.2	0.060	82.1
reflux/feed × T102407	-	-	0.000	-7119

temperature and considering that thermocouple temperature given by T102405 was being used in the model instead of T102407, the pursue of an equation to obtain T102407 from T102405 lead to the use of process historical data to create a regression that related both temperatures. The equation was obtained with a determination coefficient of 0.177 and is presented below:

$$T102405 = 73.2 - 0.09188 \times T102407 \quad (6.5)$$

In equation 6.4, T102405 was then replaced by equation 6.5 and the new water on distillate model $AARD$ was determined, its value being 69.68%. As can be seen, by replacing T102405 for equation 6.5, the $AARD$ increased more than three times. This increase is a consequence of the poor adjustment of equation 6.5 to the data which greatly increases the model's error. Although equation 6.5 can be used to replace T102405, this is not recommended as the value of water in the distillate obtained by the model would be far from reality, rendering any conclusions concerning the distillation process performance inadequate.

6.3 Fouling and steam consumption

Fouling is one of the most important factors to be taken into consideration during processes that require heat transfer, such as distillation. Being responsible for considerable losses in heat transfer, controlling and reducing fouling is always a major concern during process operation.

Different approaches exist to deal with this problem, either by preventing its formation or by its removal after forming. The first method has the advantage of preventing the problem before it sets by using certain chemicals or even removing the components responsible for the fouling. However, this solution is not always possible and removing the fouling after its formation is then required, such as in Prio Biocombustíveis S.A. case.

Removing the fouling that sets on the tubes side of the reboiler is done in two different ways, either one requiring the distillation process to stop and, therefore, all the production process. The first, and fastest, is to use a chemical CIP (clean-in-place). This method, however, when applied at the distillation column's reboiler is not 100% effective, only serving as a temporary solution before a deeper cleaning can be made. The more effective way to clean the reboiler is to open it and perform a both mechanical and chemical cleaning that leaves the reboiler free of fouling. This method, just like the first, has a major disadvantage which is the time required for its completion, which is much larger than the first method's. Considering that, to clean the reboiler, the biodiesel production has to be stopped, one can see why the time spent on cleaning is so important since longer cleaning periods lead to larger production losses.

Following what was said above, it is of the utmost importance to carefully plan when to clean the reboiler. This, however, is only possible if the evolution of fouling in this equipment can be predicted. Since it is impossible to directly measure the fouling, another indicator has to be used to assess it: the steam pressure fed to the reboiler.

Process historical data, corresponding to different production periods and different average UCO percentage incorporation in the process, for that periods, was used to study the fouling evolution in the process. The ratio between the steam pressure and column's feed flow (PV/FF) was plotted versus the reboiler operating time between cleanings. Six different periods of time, corresponding to different conditions, were identified and their corresponding graphics are presented in figure 6.2. For each graphic, a linear regression of the data was made to represent the PV/FF variation with time, which is here represented by generic "time units" (t.u).

Analysing the slopes of each graphic's regression in figure 6.2, it becomes clear that, as more UCO is incorporated in the production process, the faster PV/FF ratio rises, which is the same as saying that as more UCO is incorporated, the faster the reboiler's fouling increases. It can also be seen that, when the PV/FF ratio reaches a value close to 6×10^{-4} ,

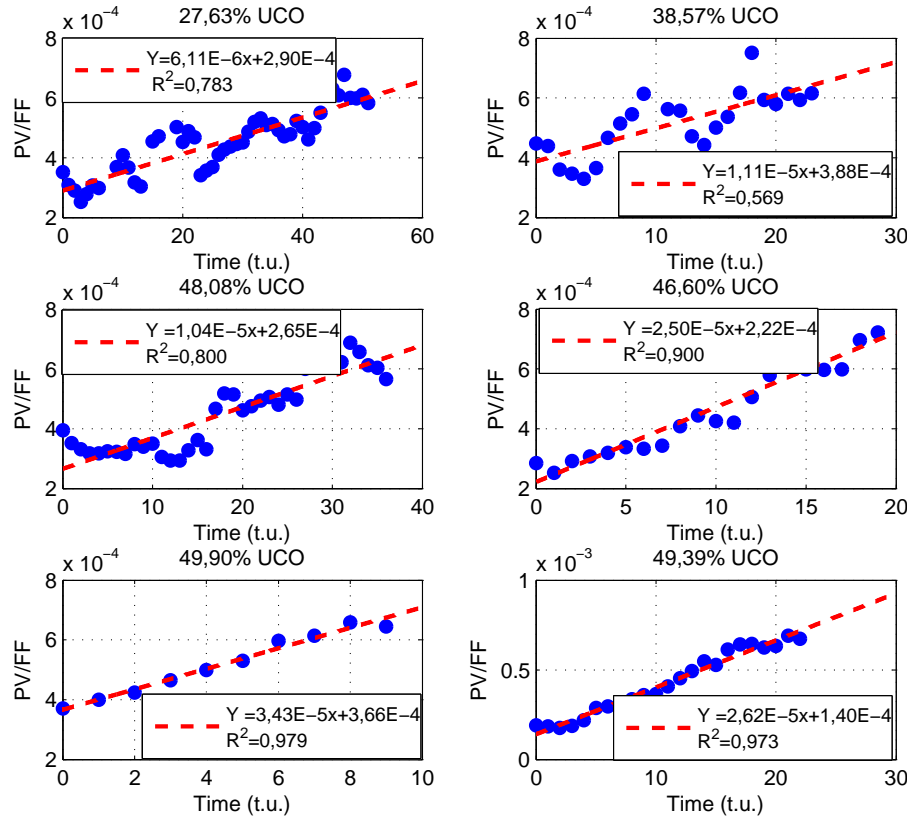


Figure 6.2: PV/FF variation with the reboiler operating time.

the distillation process is stopped and the reboiler cleaned, thus considering this value as the upper operation limit. In this figure, the lower effectiveness of the chemical CIP is also observed in the difference in initial PV/FF values of the graphics corresponding to average UCO percentages of 38.57% and 49.90% when compared to the remaining graphics that represent data collected after a both mechanical and chemical cleaning.

Another interesting characteristic of the graphics with lower average UCO percentages is their lower adjustment to the regression (R^2), which can be explained by the variation of UCO percentage incorporated during that period of time. For the last graphics, where the UCO percentage variation was much lower during the column's operating time, the overlap of the experimental points with the regression is much higher and the relationship between PV/FF *vs* time is more evident.

Using the linear regressions of each graphic in figure 6.2, the times required to reach $PV/FF = 6 \times 10^{-4}$ were determined and plotted versus the average UCO percentage, in figure 6.3, and a linear regression was implemented to create the model (equation 6.6) to determine the maximum reboiler operating time, based on the UCO percentage used. This model can now be implemented to better plan the cleaning interventions in the reboiler and, conse-

quently, reduce the excessive steam consumed by preventing the reboiler to operate at bad fouling conditions.

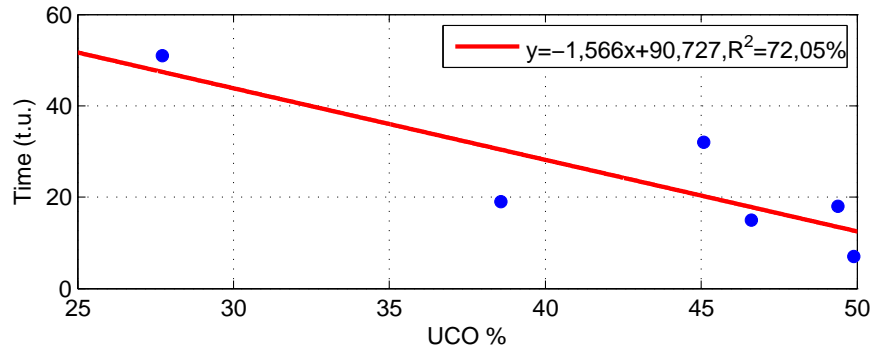


Figure 6.3: Maximum reboiler operating time variation with the UCO percentage used in the production process.

$$\text{time} = -1.566 \times \text{UCO \%} + 90.727 \quad (6.6)$$

6.3.1 Operating costs associated with fouling

As was said before, the existence of fouling in the reboiler requires larger amounts of steam to operate the column. Nonetheless, having an exact value for that extra steam cost helps to understand how financial damaging to the company can a situation like this be.

Since no flow meter to measure the steam flow to the reboiler is installed in the plant, in order to estimate it from the steam pressure, a steam flow table from the literature was used [46]. With a steam pipe nominal diameter of 150mm and considering a steam velocity of 25m/s, several values for the steam flow were used to adjust a linear equation that related the steam pressure with the steam flow. The equation obtained, as well as the steam pressure and flow values used to adjust it are presented in equation 6.7 and table 6.7, respectively.

Table 6.7: Steam flow and pressure values used to regress equation 6.7.

pressure (bar)	velocity (m/s)	pipe nominal diameter (mm)	steam flow (kg/h)
0.7	25	150	1575
1			1660
2			2520
3			3440
4			4225

$$Q_{\text{steam}} = 830.31 \times \text{PV} + 907.14 \quad (6.7)$$

Next, using process historical data from the plant's boiler (see table B.7 in appendix B), an

average value of kWh/h required to create 1kg/h of steam was determined to be 0.805kWh/kg. With this value, and the steam flow corresponding to a reboiler steam pressure of 1.5 bar and 3 bar, the steam cost was determined for a full day, being close to 1762 euros when the pressure is 1.5 bar (which is a normal steam pressure used when the reboiler is clean) and close to 2781 euros when the pressure is 3 bar (which is a pressure used when fouling is present in the reboiler). This increase of close to 58% in the steam cost required for a day of production clearly shows the economical impact that fouling has and why it should be prevented.

In light of this, a preemptive solution for the problem has been searched, in particular a solution to remove the fouling responsible components from the column's feed, such as membrane separation process. Nonetheless, due to the specific characteristics of the components to be removed and the ATEX requirements of the distillation process made it impossible to have reached a solution fast enough for it to be mentioned in this work.

Chapter 7

Conclusions and future work

The present work's study and analysis of the methanol distillation processes was made with the objective of collecting useful information that would lead to a better understanding of the process's behaviour and to develop tools to help in the control and maintenance of the said process.

Through process streams characterization, the main components in circulation, and their quantities, were determined. Although the column's feed composition changes with time, it was verified, regardless of that variation, that the distillate produced still remained within the desired limits in what regards water content, displaying process robustness and its capacity to deal with disturbances by adjusting the column's operating conditions, such as the reflux/feed ratio. The resultant impact of fouling is also visible along this work, being particularly expressive in the steam pressure increase with the operating time.

Regarding the process's simulation, Aspen Plus[®] software was used to create a computerized model of the column that simulates the process. For this simulation, the UNIQUAC thermodynamic model was used, with good results, and the missing interaction parameters for the methyl ester components were estimated using the UNIFAC model with group interaction parameters specific for fatty systems, the later also proving to be adequate for the mixture being treated. From the sensitivity analysis, made with Aspen Plus[®], the studied variables could be sorted, in a descending order, according to their influence in the distillate's purity: methanol on feed > reflux/feed ratio > reflux temperature > water on feed > reboiler outlet temperature > glycerol on feed.

The Principal Components Analysis (PCA) performed gave birth to valuable information regarding process variables interaction and their importance: Thermocouple T102404, T102405 and T102406 are positively related; Water and methanol at distillate are negatively related; Thermocouple T102409 and the methanol at residue are also negatively related; Water at feed and residue are positively related. No visible relation between the reboiler steam pressure and column's internal pressure was verified, although being expected, which can be explained by the fouling in the reboiler's tubes.

As one of this work's objectives, an empirical model to estimate the water content in the distillate, based on the reflux/feed ratio and thermocouple T102405 temperature, was obtained by Multiple Linear Regression (MLR), with an *AARD* of 19.44% and R^2 of 92.93%. This model, from the several created through a stepwise MLR, showed the best *AARD* and R^2 values, being a very useful, simple and almost effortless tool to apply in the control and management of the distillation process. Before the MLR method was implemented, a Design of Experiments method (DoE) was attempted, to retrieve experimental data, but failed since its requirements could not be kept throughout the duration of the test, therefore leading to the use of observational data instead in the MLR.

Fouling influence in the distillation process has been repeatedly mentioned, during this work, as one of the phenomenons that affect the column's performance the most. In light of its importance, a model to ascertain fouling growth, as the process operates, was made based on production history data, allowing to estimate the time which the methanol distillation column can operate before fouling reaches a point when the reboiler has to be cleaned. This tool is, like the previous, very useful as it aids in programming the reboiler's cleaning interventions.

Still regarding the reboiler's fouling, the steam costs required to operate the column for a one day period were calculated for the case when no fouling is present and when fouling is already at a critical stage, showing an increase of close to 58% in steam expenses when fouling is present. This clearly evidences the economical impact of fouling and led to the active search of a solution for this problem.

A suggestion regarding future work is, considering its domineering importance in the process, to continue the study of methods to prevent the reboiler's fouling, thus leading to considerable savings in the reboiler's steam consumption. Also, the study of the minority components in the column's feeding stream can as well prove to be useful in understanding the fouling problem and in a more in depth characterization of the process streams.

Bibliography

- [1] J.H. Clark and F. Deswarte. *Introduction to Chemicals from Biomass*. Wiley Series in Renewable Resource. Wiley, 2014.
- [2] Mikael Skou Andersen. An introductory note on the environmental economics of the circular economy. *Sustain. Sci.*, 2(1):133–140, 2007.
- [3] Steve Sorrell, Jamie Speirs, Roger Bentley, Adam Brandt, and Richard Miller. Global oil depletion: A review of the evidence. *Energy Policy*, 38(9):5290–5295, 2010.
- [4] Francesco Cherubini. The biorefinery concept: Using biomass instead of oil for producing energy and chemicals. *Energy Conversion and Management*, 51(7):1412–1421, 2010.
- [5] A. Demirbas. *Biodiesel: A Realistic Fuel Alternative for Diesel Engines*. Springer London, 2007.
- [6] R. Ulber and D. Sell. *White Biotechnology*. Advances in Biochemical Engineering / Biotechnology. Springer, 2007.
- [7] B. Kamm and M. Kamm. Principles of biorefineries. *Appl. Microbiol. Biotechnol.*, 64(2):137–145, 2004.
- [8] Palligarnai T Vasudevan and Michael Briggs. Biodiesel production—current state of the art and challenges. *J. Ind. Microbiol. Biotechnol.*, 35(5):421–430, 2008.
- [9] Fangrui Ma and Milford A. Hanna. Biodiesel production: a review1Journal Series #12109, Agricultural Research Division, Institute of Agriculture and Natural Resources, University of NebraskaLincoln.1. *Bioresource Technology*, 70(1):1–15, 1999.
- [10] European Renewable Energy Council. Renewable Energy Technology Roadmap 20% by 2020. http://www.erec.org/fileadmin/erec_docs/Documents/Publications/Renewable_Energy_Technology_Roadmap.pdf, 2008. Accessed at 2015-05-02.
- [11] D. Rajagopal, S. E. Sexton, D. Roland-Holst, and D. Zilberman. Challenge of biofuel: filling the tank without emptying the stomach? *Environ. Res. Lett.*, 2(4):044004, 2007.
- [12] Jon Van Gerpen. Biodiesel processing and production. *Fuel Process. Technol.*, 86(10):1097–1107, 2005.
- [13] Carol Lin, Lucie Anne Pfaltzgraff, Lorenzo Herrero-Davila, Egid B. Mubofu, Abderrahim Solhy, Prof James Clark, Apostolis Koutinas, Nikolaos Kopsahelis, Katerina Stamatalou, Fiona Dickson, Samarthia Thankappan, Mohamed Zahouily, Robert Brocklesby, and Rafael Luque. Food waste as a valuable resource for the production of chemicals, materials and fuels. Current situation and global perspective. *Energy Environ. Sci.*, 15:426–464, 2012.
- [14] S. Hayafuji, T. Shimidzu, S. Oh, and H. Zaima. Method and apparatus for producing diesel fuel oil from waste edible oil, October 26 1999. US Patent 5,972,057.
- [15] Ayhan Demirbas and M. Fatih Demirbas. Importance of algae oil as a source of biodiesel. *Energy Convers. Manag.*, 52(1):163–170, 2011.

- [16] A. L. Ahmad, N. H. Mat Yasin, C. J. C. Derek, and J. K. Lim. Microalgae as a sustainable energy source for biodiesel production : A review. *Renew. Sustain. Energy Rev.*, 15(1):584–593, 2011.
- [17] Ayhan Demirba. Biodiesel from vegetable oils via transesterification in supercritical methanol. *Energy Conversion and Management*, 43(17):2349–2356, 2002.
- [18] P. Ranalli. *Improvement of Crop Plants for Industrial End Uses*. SpringerLink: Springer e-Books. Springer Netherlands, 2007.
- [19] J. M. Marchetti, V. U. Miguel, and A. F. Errazu. Possible methods for biodiesel production. *Renewable and Sustainable Energy Reviews*, 11(6):1300–1311, 2007.
- [20] Ayhan Demirbas. Biodiesel production from vegetable oils via catalytic and non-catalytic supercritical methanol transesterification methods. *Progress in Energy and Combustion Science*, 31(5-6):466–487, 2005.
- [21] A.J. Dijkstra and M. Van Opstal. Process for producing degummed vegetable oils and gums of high phosphatidic acid content, October 6 1987. US Patent 4,698,185.
- [22] Anjana Srivastava and Ram Prasad. Triglycerides-based diesel fuels. *Renew. Sustain. energy Rev.*, 4(2):111–133, 2000.
- [23] Ayhan Demirbas. Biodiesel from waste cooking oil via base-catalytic and supercritical methanol transesterification. *Energy Conversion and Management*, 50(4):923–927, 2009.
- [24] Martin Kleber. Lurgi biodiesel capabilities. <http://communitybiofuels.com/references/Lurgi%20Biodiesel%20Info%20and%20References%20May%202004.pdf>.
- [25] Titipong Issariyakul, Mangesh G. Kulkarni, Lekha C. Meher, Ajay K. Dalai, and Narendra N. Bakhshi. Biodiesel production from mixtures of canola oil and used cooking oil. *Chem. Eng. J.*, 140(1-3):77–85, 2008.
- [26] S. Bari, T. H. Lim, and C. W. Yu. Effects of preheating of crude palm oil (CPO) on injection system, performance and emission of a diesel engine. *Renew. Energy*, 27(3):339–351, 2002.
- [27] L. Boros, M. L. S. Batista, Raquel V. Vaz, B. R. Figueiredo, V. F. S. Fernandes, M. C. Costa, M. A. Krahenbuhl, A. J. A. Meirelles, and J. A. P. Coutinho. Crystallization behavior of mixtures of fatty acid ethyl esters with ethyl stearate. *Energy and Fuels*, 23(9):4625–4629, 2009.
- [28] GEA Westfalia Separator Group. Trainings manual: Continuous 2-stage-neutralisation. Operating manual, 2008.
- [29] Fredrik Pomreh. Understanding and control of the methanol column 10D07. Operating manual, 2006.
- [30] D.E. Seborg, D.A. Mellichamp, T.F. Edgar, and F.J. Doyle. *Process Dynamics and Control*. John Wiley & Sons, 2010.
- [31] Anton A. Kiss and Radu M. Ignat. Enhanced methanol recovery and glycerol separation in biodiesel production - DWC makes it happen. *Applied Energy*, 99:146–153, 2012.
- [32] Mario Pagliaro, Rosaria Ciriminna, Hiroshi Kimura, Michele Rossi, and Cristina Della Pina. From glycerol to value-added products. *Angewandte Chemie - International Edition*, 46(24):4434–4440, 2007.
- [33] Fangxia Yang, Milford Hanna, and Runcang Sun. Value-added uses for crude glycerol—a byproduct of biodiesel production. *Biotechnol. Biofuels*, 5(1):13, 2012.
- [34] Martin Hájek and František Skopal. Treatment of glycerol phase formed by biodiesel production. *Bioresource Technology*, 101(9):3242–3245, 2010.

-
- [35] Instituto Portugues da Qualidade. Produtos petrolíferos. determina ção de água - método de titula ção karl fischer por coulometria. NP EN ISO 12937:200.
- [36] ASTM International. Standard test method for water using volumetric karl fischer titration. ASTM E203.
- [37] American Oil Chemists' Society. Sampling and analysis of crude glycerin - sodium periodate oxidation method. A.O.C.S. Official Method Ea-51.
- [38] European Commitee For Standardization. Fat and oil derivates - fatty acid methyl esters (fame) - determination of methanol content. EN 14110:2003.
- [39] Ming-Jer Lee, Yuan-Chen Lo, and Ho-Mu Lin. Liquidliquid equilibria for mixtures containing water, methanol, fatty acid methyl esters, and glycerol. *Fluid Phase Equilibria*, 299(2):180–190, 2010.
- [40] Hidetoshi Kuramochi, Kouji Maeda, Satoru Kato, Masahiro Osako, Kazuo Nakamura, and Shin Ichi Sakai. Application of UNIFAC models for prediction of vapor-liquid and liquid-liquid equilibria relevant to separation and purification processes of crude biodiesel fuel. *Fuel*, 88(8):1472–1477, 2009.
- [41] Gláucia F. Hirata, Charles R. A. Abreu, Larissa C. B. A. Bessa, Marcela C. Ferreira, Eduardo A. C. Batista, and Antonio J. A. Meirelles. Liquid-liquid equilibrium of fatty systems: A new approach for adjusting UNIFAC interaction parameters. *Fluid Phase Equilibria*, 360:379–391, 2013.
- [42] I.T. Jolliffe. *Principal Component Analysis*. Springer Series in Statistics. Springer, 2002.
- [43] G.J. Park. *Analytic Methods for Design Practice*. Springer London, 2007.
- [44] R. Mead, S.G. Gilmour, and A. Mead. *Statistical Principles for the Design of Experiments: Applications to Real Experiments*. Cambridge Series in Statistical and Probabilistic Mathematics. Cambridge University Press, 2012.
- [45] D.C. Montgomery, E.A. Peck, and G.G. Vining. *Introduction to linear regression analysis*. Wiley series in probability and statistics: Texts, references, and pocketbooks section. Wiley, 2001.
- [46] D.A. SNOW. *Plant Engineer's Reference Book*. Elsevier Science, 2013.
- [47] D. Green and R. Perry. *Perry's Chemical Engineers' Handbook, Eighth Edition*. McGraw Hill professional. McGraw-Hill Education, 2007.
- [48] R.M. Stephenson. *Handbook of the Thermodynamics of Organic Compounds*. Springer Netherlands, 2012.

Appendix A

Glycerol and FAME vapour pressure

The vapour pressure of glycerol, at the reboiler temperature of 111°C was estimated by the Clausius-Clapeyron relation (equation A.1).

$$\ln\left(\frac{P_1}{P_2}\right) = \frac{\Delta H_{\text{vap}}}{R} \left(\frac{1}{T_2} - \frac{1}{T_1} \right) \quad (\text{A.1})$$

- P_1 and P_2 : pressure one and pressure two, respectively (mmHg);
- T_1 and T_2 : temperature corresponding to pressure one and two, respectively (K);
- R : ideal gas constant ($\text{J} \cdot \text{K}^{-1} \cdot \text{mol}^{-1}$);
- ΔH_{vap} : latent heat of vaporization ($\text{J} \cdot \text{mol}^{-1}$)

From the literature: $P_2 = 1\text{mmHg}$ [47], $T_2 = 398.65\text{(K)}$ [47] and $\Delta H_{\text{vap}} = 85800\text{J} \cdot \text{mol}^{-1}$ [48]. Applying these to equation A.1, the value of P_1 at $T_1 = 111\text{(C)} = 384.15\text{(K)}$ is determined:

$$\ln\left(\frac{P_1}{1}\right) = \frac{85800}{8.314} \left(\frac{1}{398.65} - \frac{1}{384.15} \right) \Leftrightarrow P_1 = 0.376\text{mmHg} \quad (\text{A.2})$$

The vapour pressure for FAMEs was calculated using Antoine equation (equation A.3).

$$\log_{10} P_{\text{vap}} = A - [B/(C + T)] \quad (\text{A.3})$$

The Antoine equation parameters used aswell as the results for the vapour pressure (bar) can be found in table A.1. The temperature used is in K.

Table A.1: Antoine equation parameters

	A	B	C	P_{vap} (bar)
methyl palmitate	6.247	3709.672	-1.062	3.66×10^{-4}
methyl oleate	5.225	2723.181	-91.822	8.12×10^{-5}
methyl linoleate	3.828	2066.995	-116.870	1.24×10^{-4}

Appendix B

Stream compositions and column's operating data

In the following tables, the process data collected during this work is presented. For glycerol and the “others”, their stream's mass fractions were only measured until 15-06-2015. A scheme from the distillation column (figure B.1) is also presented here, showing the relative position of the temperature and pressure indicators in the column.

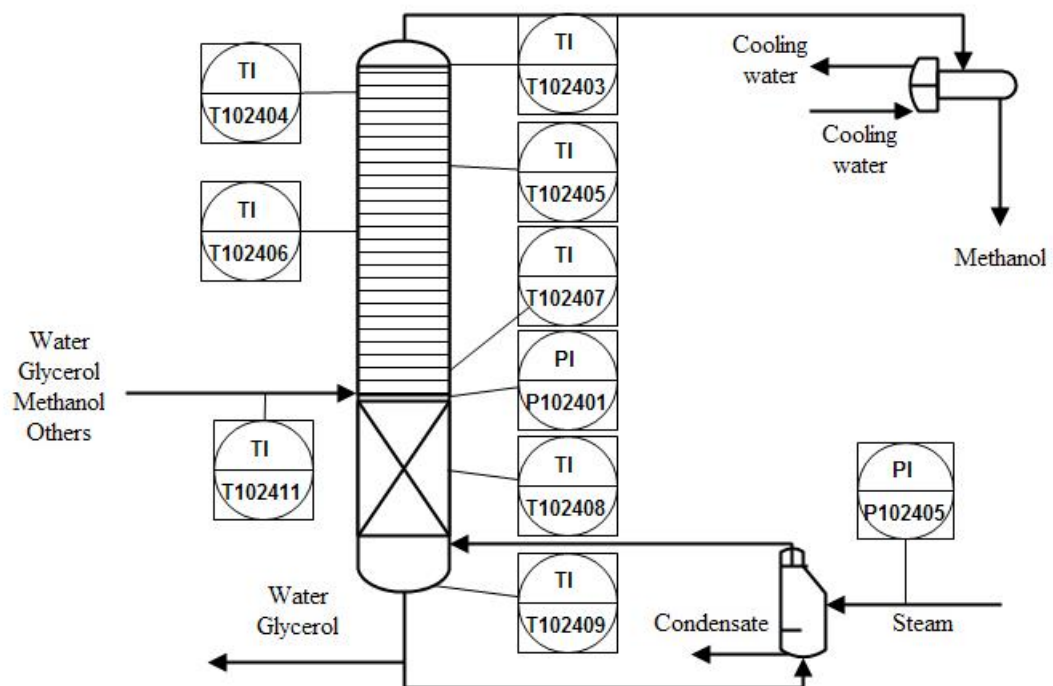


Figure B.1: Distillation column with the different temperature and pressure indicators relative location along the column.

Table B.1: Mass fraction composition (%) of glycerol, water, methanol and “others” in Stream A (from tank 10F08)

day	glycerol	water	methanol	“others”
10-02-2015	24.134	52.13	22.953	0.7836
11-02-2015	23.702	51.36	22.866	2.0716
13-02-2015	26.198	51.729	21.877	0.1952
16-02-2015	23.691	53.031	22.236	1.0417
23-02-2015	22.222	55.34	20.223	2.2152
24-02-2015	20.277	56.176	22.05	1.4976
25-02-2015	23.248	54.349	20.53	1.8729
26-02-2015	23.444	47.038	22.811	6.7064
27-02-2015	25.307	41.628	26.249	6.8166
02-03-2015	23.395	45.696	22.821	8.0881
03-03-2015	22.365	47.041	22.85	7.7446
09-03-2015	24.295	45.579	23.972	6.153
10-03-2015, 10:00	24.261	45.602	22.773	7.3641
10-03-2015, 12:00	23.927	46.069	24.231	5.7735
10-03-2015, 17:00	24.275	45.891	23.428	6.4066
10-03-2015, 19:00	23.99	45.962	23.305	6.7431
12-03-2015	23.564	47.129	21.715	7.5921
19-03-2015	23.096	48.192	23.044	5.6678
08-04-2015	22.985	51.286	23.253	2.4762
03-06-2015, 09:00	23.891	50.631	21.392	4.086
03-06-2015, 09:30	23.626	50.344	21.902	4.1276
03-06-2015, 12:00	22.507	50.848	21.457	5.1888
03-06-2015, 12:30	22.314	51.753	21.101	4.8321
03-06-2015, 17:00	23.131	52.341	21.811	2.7166
03-06-2015, 17:30	23.764	51.23	20.858	4.1476
08-06-2015	21.99	50.435	23.954	3.6204
09-06-2015	23.658	52.426	22.443	1.4739
11-06-2015	22.982	53.82	21.574	1.6228
15-06-2015	23.371	54.266	21.843	0.5203
25-06-2016, 14:30	-	52.901	21.828	-
25-06-2015, 16:30	-	51.242	21.064	-
26-06-2015	-	52.353	21.876	-
29-06-2015, 15:00	-	52.753	19.847	-
29-06-2015,18:30	-	52.663	20.065	-

APPENDIX B. STREAM COMPOSITIONS AND COLUMN'S OPERATING DATA

30-06-2015	-	52.9	20.074	-
01-07-2015	-	52.251	20.43	-
02-07-2015	-	53.438	20.749	-
03-07-2015	-	53.226	21.556	-
07-07-2015	-	53.735	19.905	-
09-07-2015	-	55.306	20.355	-
13-07-2015	-	51.265	20.983	-
15-07-2015	-	52.43	20.006	-
16-07-2015	-	52.229	19.987	-
17-07-2015	-	51.897	21.023	-
20-07-2015	-	53.477	19.808	-
21-07-2015	-	53.031	20.892	-
22-07-2015	-	53.833	21.065	-
24-07-2015	-	53.83	19.587	-
18-08-2015	-	54.036	20.046	-

Table B.2: Mass fraction composition (%) of glycerol, water, methanol and “others” in Stream D (from the bottom of the distillation column)

day	glycerol	water	methanol	“others”
10-02-2015	30.131	68.5301	0.334666667	1.004
11-02-2015	29.243	67.16125	0.356666667	3.2395
13-02-2015	29.187	68.83145	0.3575	1.6245
16-02-2015	30.236	66.9134	0.2673	2.5831
23-02-2015	27.563	70.6252	0.398266667	1.413
24-02-2015	26.889	70.15825	0.4838	2.4691
25-02-2015	28.022	70.23275	0.366666667	1.3789
26-02-2015	29.363	61.447	0.350166667	8.8397
27-02-2015	32.71	56.7846	0.620866667	9.8842
02-03-2015	29.808	59.5545	0.5314	10.106
03-03-2015	28.841	61.0004	0.491933333	9.6668
09-03-2015	30.866	59.48725	0.2934	9.3536
10-03-2015, 10:00	30.172	59.54665	0.3565	9.9253
10-03-2015, 12:00	30.065	60.05705	0.189433333	9.6888
10-03-2015, 17:00	30.5	60.90745	0.093333333	8.4993
10-03-2015, 19:00	30.258	60.4846	0.224133333	9.0331
12-03-2015	29.175	61.7367	0.22	8.8679

19-03-2015	29.204	63.52745	0.3306	6.9375
08-04-2015	29.332	66.6094	0.178766667	3.8795
03-06-2015, 09:00	27.994	64.7008	0.5326	6.7729
03-06-2015, 09:30	29.441	64.5438	0.53895	5.4761
03-06-2015, 12:00	28.285	64.96905	0.48145	6.2647
03-06-2015, 12:30	29.148	64.4203	0.42565	6.0063
03-06-2015, 17:00	29.013	65.0884	0.44945	5.4493
03-06-2015, 17:30	29.118	64.7868	0.4008	5.6944
08-06-2015	29.271	63.584	0.7816	6.3629
09-06-2015	30.711	67.65335	0.72005	0.9159
11-06-2015	29.951	69.12945	0.2515	0.6683
15-06-2015	29.594	68.61385	0.5156	1.2762
25-06-2016, 14:30	-	66.71675	0.59045	-
25-06-2015, 16:30	-	67.1372	0.65295	-
26-06-2015	-	67.1457	0.64885	-
29-06-2015, 15:00	-	66.36515	0.54525	-
29-06-2015,18:30	-	65.5677	0.75675	-
30-06-2015	-	67.38455	0.74275	-
01-07-2015	-	66.41895	0.63135	-
02-07-2015	-	67.72195	0.42065	-
03-07-2015	-	68.77665	0.4885	-
07-07-2015	-	68.3911	0.3814	-
09-07-2015	-	70.06575	0.4936	-
13-07-2015	-	65.134	0.57885	-
15-07-2015	-	65.0422	0.7838	-
16-07-2015	-	65.3747	0.7368	-
17-07-2015	-	65.89205	0.5807	-
20-07-2015	-	65.9481	0.99385	-
21-07-2015	-	67.38395	0.805	-
22-07-2015	-	68.5819	0.42755	-
24-07-2015	-	69.2929	0.46035	-
18-08-2015	-	69.9557	0.24695	-

Table B.3: Mass fraction composition (%) of water and methanol in Stream C (from tank 10F06)

day	water	methanol
10-02-2015	0.0153	99.985
11-02-2015	0.0324	99.968
13-02-2015	0.0212	99.979
16-02-2015	0.0184	99.982
23-02-2015	0.0138	99.986
24-02-2015	0.0088	99.991
25-02-2015	0.0209	99.979
26-02-2015	0.0203	99.98
27-02-2015	0.0228	99.977
02-03-2015	0.0755	99.924
03-03-2015	0.0976	99.902
09-03-2015	0.0425	99.958
10-03-2015, 10:00	0.0202	99.98
10-03-2015, 12:00	0.0536	99.946
10-03-2015, 17:00	0.0167	99.983
10-03-2015, 19:00	0.0393	99.961
12-03-2015	0.0394	99.961
19-03-2015	0.0416	99.958
08-04-2015	0.0185	99.982
03-06-2015, 09:00	0.027	99.973
03-06-2015, 09:30	0.0228	99.977
03-06-2015, 12:00	0.0173	99.983
03-06-2015, 12:30	0.0167	99.983
03-06-2015, 17:00	0.0119	99.988
03-06-2015, 17:30	0.016	99.984
08-06-2015	0.0537	99.946
09-06-2015	0.0965	99.904
11-06-2015	0.081	99.919
15-06-2015	0.0152	99.985
25-06-2016, 14:30	0.0146	99.985
25-06-2015, 16:30	0.0114	99.989
26-06-2015	0.0249	99.975
29-06-2015, 15:00	0.0217	99.978
29-06-2015,18:30	0.0197	99.98

30-06-2015	0.0259	99.974
01-07-2015	0.0298	99.97
02-07-2015	0.0309	99.969
03-07-2015	0.0418	99.958
07-07-2015	0.0241	99.976
09-07-2015	0.036	99.964
13-07-2015	0.0269	99.973
15-07-2015	0.0144	99.986
16-07-2015	0.0296	99.97
17-07-2015	0.047	99.953
20-07-2015	0.0464	99.954
21-07-2015	0.0584	99.942
22-07-2015	0.0916	99.908
24-07-2015	0.0529	99.947
18-08-2015	0.0156	99.984

Table B.4: Methanol distillation column's operating data.

day	feed (kg/h)	residue (kg/h)	distillate (kg/h)	reflux (kg/h)	reflux (%)	HCL stream (37%) (kg/hr)
10-02-2015	5319.9	4204.01	1207.2	1925.8	0.362	91.29
11-02-2015	5047.45	3990.34	1140.3	1755.8	0.3479	83.2
13-02-2015	5039.05	4030.45	1088.2	1784.7	0.3542	79.64
16-02-2015	5076.9	4042.52	1118.3	1784.7	0.3515	83.94
23-02-2015	5319.39	4341.91	1058.6	1861.1	0.3499	81.11
24-02-2015	5339.56	4260.18	1156.9	1853.1	0.3471	77.48
25-02-2015	5352.68	4269.2	1083.5	1894.5	0.3539	0
26-02-2015	5438.99	4212.8	1226.2	1914.9	0.3521	0
27-02-2015	4949.69	3763.9	1276.2	1594.1	0.3221	90.36
02-03-2015	5149.21	4086.6	1154.3	1618.5	0.3143	91.64
03-03-2015	5100.26	4036.74	1146.7	1622.8	0.3182	83.15
09-03-2015	5210.02	4058.64	1237.6	1686.1	0.3236	86.2
10-03-2015, 10:00	5179.05	4101.16	1165.1	1696.1	0.3275	87.17
10-03-2015, 12:00	5182.4	4021.38	1248.8	1698.8	0.3278	87.78
10-03-2015, 17:00	5179.9	4060.01	1210	1914.1	0.3695	90.06
10-03-2015, 19:00	5184.72	4074.79	1199.7	1915	0.3694	89.72
12-03-2015	5094.54	4081.39	1097.7	1664.4	0.3267	84.58

APPENDIX B. STREAM COMPOSITIONS AND COLUMN'S OPERATING DATA

19-03-2015	5191.2	4096.89	1183.2	1695.7	0.3266	88.9
08-04-2015	5110.81	4015.95	1181.4	1826.2	0.3573	86.58
03-06-2015, 09:00	5466.07	4408.44	1146.1	1743.3	0.3189	88.5
03-06-2015, 09:30	5480.27	4393.03	1176.9	1745.6	0.3185	89.65
03-06-2015, 12:00	5476.39	4409.6	1154	1861	0.3398	87.24
03-06-2015, 12:30	5433.39	4394.52	1128	1846.3	0.3398	89.12
03-06-2015, 17:00	5441.65	4368.7	1167.4	1952.8	0.3589	94.44
03-06-2015, 17:30	5436.52	4407.66	1116.5	1959.5	0.3604	87.61
08-06-2015	5200.87	4057.42	1214.8	1514	0.2911	71.3
09-06-2015	5478.23	4368.28	1199.2	1574	0.2873	89.22
11-06-2015	4302.46	3454.74	920.29	1324	0.3077	72.57
15-06-2015	5379.93	4315.61	1153.1	1654.1	0.3074	88.73
25-06-2016, 14:30	5196.89	4177.28	1109.9	1773.6	0.3413	90.28
25-06-2015, 16:30	5230.78	4251.16	1074.2	1782.8	0.3408	94.56
26-06-2015	5100.37	4089.31	1089.5	1634.3	0.3204	78.45
29-06-2015, 15:00	4697.03	3864.71	911.36	1517	0.323	79.04
29-06-2015,18:30	5189.5	4264.44	1009.2	1587.4	0.3059	84.13
30-06-2015	5350.32	4390.67	1041.7	1578.8	0.2951	82.02
01-07-2015	5331.12	4355.38	1062	1598	0.2998	86.24
02-07-2015	5262.4	4309.43	1074.1	1573.8	0.2991	121.14
03-07-2015	5456.17	4389.68	1155.2	1650.4	0.3025	88.66
07-07-2015	4866.75	3991.16	953.74	1507	0.3097	78.15
09-07-2015	5320.09	4344.49	1061.8	1655.8	0.3112	86.23
13-07-2015	4597.55	3741.75	943.28	1424.9	0.3099	87.48
15-07-2015	4596.61	3777.62	890.13	1419	0.3087	71.14
16-07-2015	4651.92	3823.17	901.86	1412.7	0.3037	73.11
17-07-2015	4455.13	3610.13	916.07	1356.2	0.3044	71.07
20-07-2015	4572.65	3776.79	868.64	1295.4	0.2833	72.78
21-07-2015	4444.27	3610.94	899.94	1257	0.2828	66.61
22-07-2015	4399.68	3548.97	912.46	1309.8	0.2977	61.75
24-07-2015	4469.48	3675.2	858.96	1323.2	0.2961	64.68
18-08-2015	5072.97	4145.97	1006.9	1799.9	0.3548	79.87

Table B.5: Column's thermocouples T102404, T102405, T102406, T102407, T102408 and T102509 temperatures.

	thermocouple temperature					
day	T102404 (°C)	T102405 (°C)	T102406 (°C)	T102407 (°C)	T102408 (°C)	T102409 (°C)
10-02-2015	65.29	65.84	67.79	80.28	96.46	103.51
11-02-2015	65.34	66.06	69	80.18	96.11	102.95
13-02-2015	65.33	65.8	67.74	80.14	96.06	103.3
16-02-2015	65.4	66.02	68.57	80.61	96.85	103.75
23-02-2015	65.24	65.73	67.61	79.59	94.01	102.52
24-02-2015	65.53	65.92	67.3	79.03	93.38	102.4
25-02-2015	65.61	66.17	68.29	79.86	94.62	103.14
26-02-2015	65.57	66.17	68.5	79.99	96.06	103.58
27-02-2015	65.5	66.05	67.89	77.6	91.09	101.48
02-03-2015	65.73	66.78	70.52	80.13	92.65	101.68
03-03-2015	65.82	67.18	71.62	80.66	93.93	102
09-03-2015	65.44	66.1	68.72	81.39	97.07	103.52
10-03-2015, 10:00	65.34	65.84	67.41	79.19	94.46	103.11
10-03-2015, 12:00	65.53	66.39	69.73	81.97	97.4	104.17
10-03-2015, 17:00	65.39	65.94	68.21	82.04	99.58	105.12
10-03-2015, 19:00	65.33	65.67	66.57	78.19	95.99	104.15
12-03-2015	65.42	66.08	68.56	80.56	95.4	103.63
19-03-2015	65.28	66.19	66.9	80	95.08	102.9
08-04-2015	65.27	65.84	67.76	81.19	100.3	104.55
03-06-2015, 09:00	65.22	65.75	67.45	78.18	93.67	102.84
03-06-2015, 09:30	65.22	65.78	67.46	78.14	93.77	102.8
03-06-2015, 12:00	65.22	65.68	66.9	77.84	94.32	103.17
03-06-2015, 12:30	65.22	65.66	66.95	77.96	94.49	103.36
03-06-2015, 17:00	65.17	65.54	66.38	76.9	94.33	103.15
03-06-2015, 17:30	65.19	65.53	66.38	76.75	94.79	103.48
08-06-2015	65.3	66.11	68.55	77.7	92.87	101.34
09-06-2015	65.4	66.48	69.48	78.11	92.2	100.92
11-06-2015	65.27	66.2	69.43	81.82	95.38	103.39
15-06-2015	65.15	65.65	66.71	77.73	97.89	102.22
25-06-2016, 14:30	65.25	65.63	66.28	76.38	97.58	102.4
25-06-2015, 16:30	65.24	65.65	66.32	76.68	97.63	102.45
26-06-2015	65.32	65.67	66.64	77.72	97.12	101.99

APPENDIX B. STREAM COMPOSITIONS AND COLUMN'S OPERATING DATA

29-06-2015, 15:00	65.08	65.51	66.47	77.55	97.99	102.15
29-06-2015,18:30	65.09	65.55	66.56	77.01	96.35	100.82
30-06-2015	65.1	65.63	67.16	78.55	96.65	100.95
01-07-2015	65.1	65.68	67.32	78.03	97.19	101.57
02-07-2015	65.3	65.89	67.55	78.06	96.96	101.97
03-07-2015	65.33	66.05	68.23	78.58	97.98	102.63
07-07-2015	65.23	65.86	67.72	77.45	96.77	102.9
09-07-2015	65.16	65.83	67.99	77.53	95.21	95.21
13-07-2015	65.23	65.81	67.62	76.67	93.81	102.03
15-07-2015	65.09	65.56	66.72	76.29	92.69	100.55
16-07-2015	65.16	65.69	67.3	76.68	93.27	100.72
17-07-2015	65.27	66.01	68.36	77.29	95.05	101.62
20-07-2015	65.19	65.89	67.96	77.01	92.34	99.79
21-07-2015	65.33	66.07	68.51	77.37	92.62	100.08
22-07-2015	65.48	65.5	69.72	79.06	97.07	102.4
24-07-2015	65.29	66.05	68.94	79.02	96.98	102.38
18-08-2015	65.08	65.47	66.58	79.9	98.13	103.81

Table B.6: Column's thermocouple T102403, feed and reflux temperatures and reboiler's steam (P102405) and internal pressures (P102401).

	temperature			pressure	
	T102403	feed	reflux	P102401	P102405
day	(°C)	(°C)	(°C)	(mbarg)	(bar)
10-02-2015	65.3	74.74	-	83.97	2.43
11-02-2015	65.28	74.5	-	78.24	2.22
13-02-2015	65.37	74.48	-	78.99	2.59
16-02-2015	65.41	74.58	-	78.18	2.64
23-02-2015	65.28	74.62	-	79.4	2.51
24-02-2015	65.61	74.62	-	82.87	3
25-02-2015	65.66	74.77	-	81.25	3
26-02-2015	65.6	77.88	22.7	83.68	3
27-02-2015	65.51	77.8	24.7	78.07	3.08
02-03-2015	65.55	75.69	30.6	74.07	3.1
03-03-2015	65.51	77.67	29.8	73.72	3.1
09-03-2015	65.38	74.91	25.1	73.44	1.91
10-03-2015, 10:00	65.43	74.96	29	73.72	1.71

10-03-2015, 12:00	65.42	74.9	29.9	74.42	1.75
10-03-2015, 17:00	65.38	75.06	29.8	78.82	1.9
10-03-2015, 19:00	65.38	74.97	29.4	80.21	1.85
12-03-2015	65.36	75.01	28.9	72.16	1.72
19-03-2015	65.17	87.15	30.3	75	2.91
08-04-2015	65.3	74.97	29.4	79.22	1.66
03-06-2015, 09:00	65.28	74.72	30.4	77.78	2.63
03-06-2015, 09:30	65.31	75.02	32.1	77.8	2.62
03-06-2015, 12:00	65.32	74.67	32	80.44	2.76
03-06-2015, 12:30	65.31	74.59	32.1	80.26	2.75
03-06-2015, 17:00	65.32	74.66	31.9	82.81	2.8
03-06-2015, 17:30	65.28	74.64	32.4	83.74	2.82
08-06-2015	65.26	74.63	35.5	72.39	2.99
09-06-2015	65.25	74.49	35.8	73.44	3.11
11-06-2015	65.16	76.62	29.9	71.18	3.19
15-06-2015	65.33	74.63	34.5	75.17	2.16
25-06-2016, 14:30	65.37	74.68	32.8	79.4	1.14
25-06-2015, 16:30	65.38	74.74	31.8	79.86	1.13
26-06-2015	65.5	74.64	32.7	77.89	0.95
29-06-2015, 15:00	65.27	74.41	35.5	70.89	1.09
29-06-2015,18:30	65.28	74.5	35.5	72.91	1.31
30-06-2015	65.24	74.54	33.7	75.17	1.5
01-07-2015	65.26	74.44	34.3	73.9	1.55
02-07-2015	65.41	74.48	33.8	72.45	1.58
03-07-2015	65.37	74.56	33.2	75.52	1.86
07-07-2015	65.36	74.44	33.2	70.89	2.4
09-07-2015	65.23	74.56	36.6	102.82	2.76
13-07-2015	65.37	75.64	32.2	69.73	3.03
15-07-2015	65.25	75.57	33.2	69.56	2.79
16-07-2015	65.31	76.74	33.1	71.47	3.15
17-07-2015	65.27	76.7	34.3	70.31	3.13
20-07-2015	65.3	76.62	33.5	69.5	3.12
21-07-2015	65.35	77.67	32.9	68.4	3.11
22-07-2015	65.4	77.64	32	70.31	3.12
24-07-2015	65.31	77.75	31.2	71.18	3.13
18-08-2015	65.27	74.82	32	81.6	1.68

Table B.7: Boiler steam production and respective daily energy consumption.

day	Steam flow (kg/h)			daily kWh consumption
	00h00	8h00	16h00	
1	4214.9	4244.4	4234.9	79495
4	4415.8	4490.3	4529.3	84546
8	4362.4	4503.7	4741.2	87152
9	4518.7	4582	4457.1	85573
10	4419.3	4399.1	4370.2	84879
11	4290.2	4393.9	4204.9	84742
12	4434	4680.6	4681	83902
14	4464.2	4116	4142.1	86636
15	4062.6	4175.1	3934.4	80959
19	4191.6	4213.2	4197.4	80775
20	4194.1	4270.3	4241.4	81872
22	4677.4	4652.5	4786.7	92872
23	4842.7	4527.3	4714.4	90990
24	3844.6	4154.8	3908.5	84139
25	4556.6	4244.1	4677.5	78807